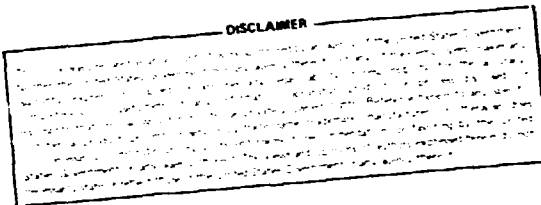


Master



ORNL/MIT-312

Contract No. W-7405-eng-26

ENVIRONMENTAL SCIENCES DIVISION

MACROPORE-MESOPORE MODEL OF WATER FLOW THROUGH AGGREGATED POROUS MEDIA

L. Fong
H.R. Appelbaum

Consultants:
R.J. Luxmoore and G.T. Yeh

Date Published - December 1980

Oak Ridge Station
School of Chemical Engineering Practice
Massachusetts Institute of Technology
K.J. Fallon, Director

Oak Ridge National Laboratory
Oak Ridge, Tennessee 37830
Operated by
Union Carbide Corporation
for the
Department of Energy

ABSTRACT

A combined, one-dimensional, macropore-mesopore, hydrologic model was developed for simulating water flow through soils for analysis of data related to water and chemical flow in soils. Flows within the macroporous system as well as interactive flows between macroporous and mesoporous systems were modeled. Computer subroutines were written and incorporated into the existing one-dimensional Terrestrial Ecosystem Hydrologic Model (TEHM) developed at ORNL. Simulation showed that macropore flow effects are important during heavy precipitation and are more significant in soils of comparatively low hydraulic conductivity (5 - 10 cm/d). Increased drainage and decreased lateral flow result from the addition of the macropore model. The effect was more pronounced in soils of large macroporosity. Preliminary results indicate that the model is insensitive to geometrical properties of macropores.

Contents

	<u>Page</u>
1. Summary	1
2. Introduction	1
2.1 Background	1
2.2 Objective and Approach	2
3. Conceptual Model	2
3.1 Geometry of Pores	2
3.2 Porosity	3
3.3 Flow Equations	3
3.4 Configurations of Pores and Flow Interactions	3
4. Existing Model	5
5. Computer Programs	8
6. Evaluation and Sensitivity Analysis	8
7. Conclusions	20
8. Recommendations	20
9. Acknowledgments	21
10. Appendix	22
10.1 Computer Logic	22
10.2 Computer Programs and Sample Output	23
10.3 Definition of Calculated Terms in Programs	23
10.4 Calculation of Maximum Flow Rate Through Macropores	32
10.5 Pore-Size Distribution	34
10.6 Documentation of Inputs	46
10.7 Input Data Sets	48
10.8 Computer Variables	50
10.9 Nomenclature	52
10.10 Literature Cited	53
10.11 Literature Surveyed	54

1. SUMMARY

Flow of water through macropores in soil, for which capillary effects are negligible, has important implications toward water-pollution control, waste treatment, and irrigation. Existing models, simulating only mesoporous flow, show significant discrepancies between calculated results and field data. A model was developed to account for macroporous flow within the framework of the existing one-dimensional Terrestrial Ecosystem Hydrologic Model (TEHM) (3).

The expanded model is employed for hydrologic scenarios involving ponding, saturated mesopores, or existing water in macropores. Water infiltrates through the top two layers of macropores, with excess water considered as surface runoff. Flow from mesopores to macropores is simulated when mesopores are saturated. When mesopores are unsaturated, water flows to them from macropores. Flow is assumed to be controlled by mesopores and governed by Darcy's Law. Any excess flow from macropores is considered to be lateral flow. Additional inputs to the model are volumes of macroporosity, pore dimensions, and volumes of dead-end macropores.

Simulation has focused on sensitivity of flow to hydraulic conductivity and macroporosity. For soils of high hydraulic conductivity (120 - 240 cm/d), the macropore effect is not significant, even for a macroporosity of 0.08. Infiltrated water occurs mostly as drainage from mesopores, while both lateral flow and surface runoff are negligible. On the other hand, macropores play a significant role in soils of low hydraulic conductivity (5 - 10 cm/d). An increase in macroporosity results in an increase in drainage and a decrease in lateral flow. Macropore flow effects are readily observed in the daily flow patterns within and between the mesoporous and macroporous systems. A comparison of infiltration and water-content curves for soil under heavy and light precipitation also confirmed the importance of macropores during heavy rainfall.

2. INTRODUCTION

2.1 Background

The phenomena associated with fluid flow through aggregated porous media must be considered to properly understand soil hydrology, enhanced petroleum recovery, and management of waste-disposal sites. Of special interest to this project is the bulk flow of water through soil. There is evidence that classical models based on Darcy's Law are inadequate to simulate the flow, since in many cases they produce unacceptably low infiltration rates, depths of chemical penetration, and rapid drop of water potential gradients. Clearly, a more realistic hydrodynamic model is desirable.

Several investigators (2, 5, 6, 9) concluded that a significant amount of water flows through large channels, or macropores, for which capillary effects are negligible. This channeling diverts water from the more extensive network of mesopores and becomes particularly important when surface ponding arises, during heavy rainfall, or when subsurface ponding (perched water table) occurs in winter. Macropores are defined as being water-filled at water potentials greater than -10 mbar, and mesopores are defined as being water-filled in the water potential range from -100 to -10 mbar. Beven and Germann (1) present a one-dimensional model of bulk flow in a combined mesopore/macropore system. The flow in mesoporous and macroporous systems was considered along with the interaction flow between them. Distributions of cylindrical pores and rectangular slits were adapted for the geometry of the macropores. Equations of laminar flow, based on Poiseuille's Law, were used to model the macroporous system. The presence of macropores increased overall losses to infiltration, with the effect being greatest for soils of intermediate hydraulic conductivities. However, this model was too complicated for direct application to our project.

2.2 Objective and Approach

The Environmental Sciences Division at Oak Ridge National Laboratory has developed a one-dimensional, Terrestrial Ecosystem Hydrologic Model (TEHM) (3) for simulating mesoporous flow of water in soils. The model was tested and illustrated by field data from the Walker Branch Watershed. The goal of this project was to develop a model to account for the macroporous flow and then to incorporate it into the TEHM computer model. First, a conceptual model of the combined macropore/mesopore system was developed. Then subroutines that were compatible with TEHM were written to simulate the flow in the macropores and the interactive flow between macropores and mesopores. Finally, the combined model was tested with field data and a sensitivity analysis was conducted.

3. CONCEPTUAL MODEL

A conceptual model of the macroporous system was developed, based on suggestions by R.J. Luxmoore (4), observation of the field samples, and the literature review. Geometry of pores, pore-size distribution and definition, porosity, and flow equations were considered.

3.1 Geometry of Pores

A theoretical soil profile has three main horizons, identified in order of depth as A, B, and C. The A-horizon, which extends about 30 cm into the soil, contains more sand and silt than the subsequent layers. Its macropores arise largely from biological forces such as roots and worm-holes. The B-horizon contains more clay than the A-horizon and can

extend from 30 to 180 cm into the soil. The macropores are caused mainly by physical forces, such as the expansion and shrinkage of aggregated soil particles.

The A- and B-horizons were of primary concern in our model. The shape of the macropores in those two layers was determined according to the nature of the pores. Cylindrical pores were assumed to be predominant in the A-horizon, as opposed to rectangular cracks in the B-horizon. The pore-size distribution was also analyzed but was not directly applied to the model. Results of that work are described in Appendix 10.5.

3.2 Porosity

An average value for mesoporosity was estimated to be 0.5 ml/ml for soils in both A- and B-horizons, based on findings in the literature (10). As noted above, mesoporosity can be obtained from the change in water content at soil water potentials less than -10 mbar (Fig. 14 in Appendix 10.5). Macroporosity may vary considerably, even for the same soil, due to its random nature. Its value was estimated to be 0.01 to 0.05 ml/ml in the literature (1). An appropriate value was obtained from the field data by assuming that macroporous flow was dominant whenever soil water potential was greater than -10 mbar (see Fig. 14). The change in water content for this range gave macroporosities of 0.05 to 0.15 ml/ml for different depths in the soil block study on the Walker Branch Watershed.

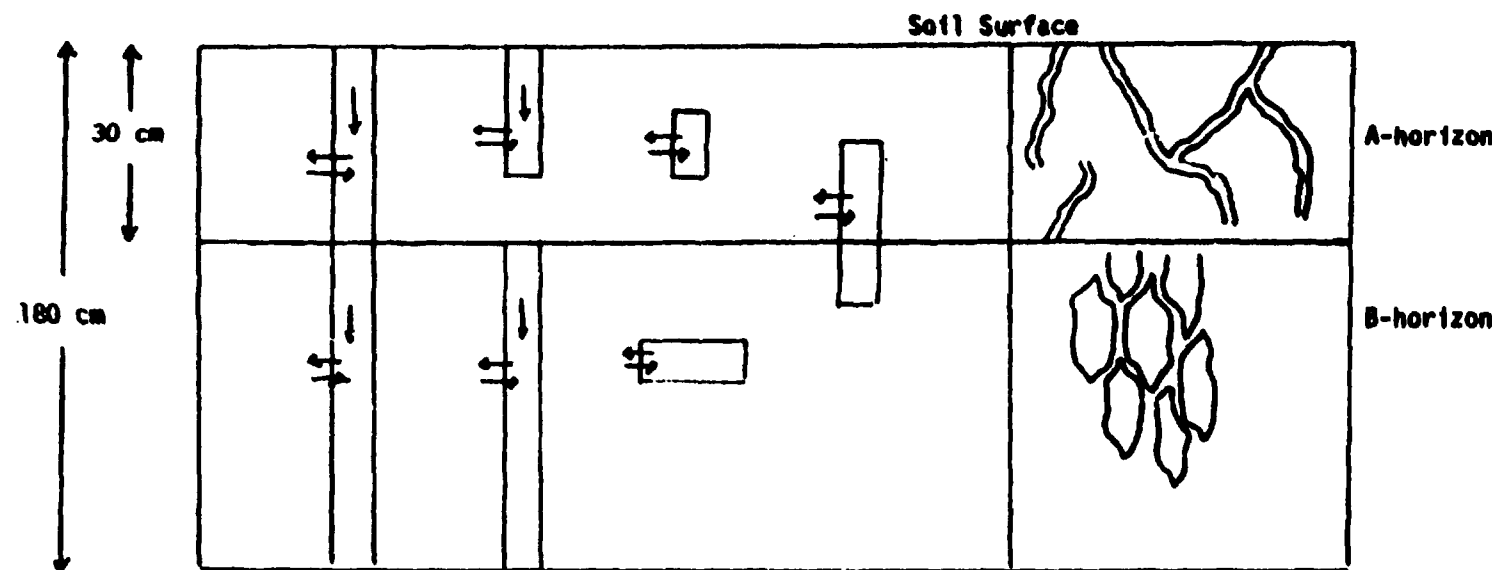
3.3 Flow Equations

Flow equations in an annulus and in a slit were adapted for cylindrical pores and rectangular cracks, respectively. The maximum flow rate allowed in both configurations was calculated for a range of sizes, as shown in Appendix 10.4. An average precipitation rate was at least three orders of magnitude smaller than the maximum flow rate through the macropores, which justified the assumption that flow in the pores was not constrained by pore configuration but rather by pore capacity.

3.4 Configurations of Pores and Flow Interactions

Both continuous and dead-end macropores were considered in the model. The different configurations are shown in Fig. 1.

During surface ponding, infiltration entered the macropores until the macropore capacity of the top two layers was exceeded; the excess was considered as surface runoff. Within each layer, flow from mesopores to macropores was simulated when the mesopores were saturated; flow from macropores to unsaturated mesopores was modeled when the macropores contained water. Only amounts above mesopore saturation were allowed to flow into the



MASSACHUSETTS INSTITUTE OF TECHNOLOGY
 SCHOOL OF CHEMICAL ENGINEERING PRACTICE
 AT
 OAK RIDGE NATIONAL LABORATORY

MACROPORES IN SOIL
 WITH MESOPORE INTERACTION

DATE 5-5-80	DRAWN BY LF	FILE NO. CEPS-X-312	FIG. 1
----------------	----------------	------------------------	-----------

macropores. The macropore-to-mesopore flow was modeled as Darcy flow, which was mesopore-controlled:

$$Q = KA \frac{d\psi}{dx} \quad (1)$$

where

Q = flux of water, $\text{cm}^3/\text{cm}^2\text{-d}$

K = hydraulic conductivity of soil, cm/d

ψ = hydraulic potential between macropores and mesopores, cm water

x = average distance between macropores and mesopores, cm

A = area of interaction, cm^2

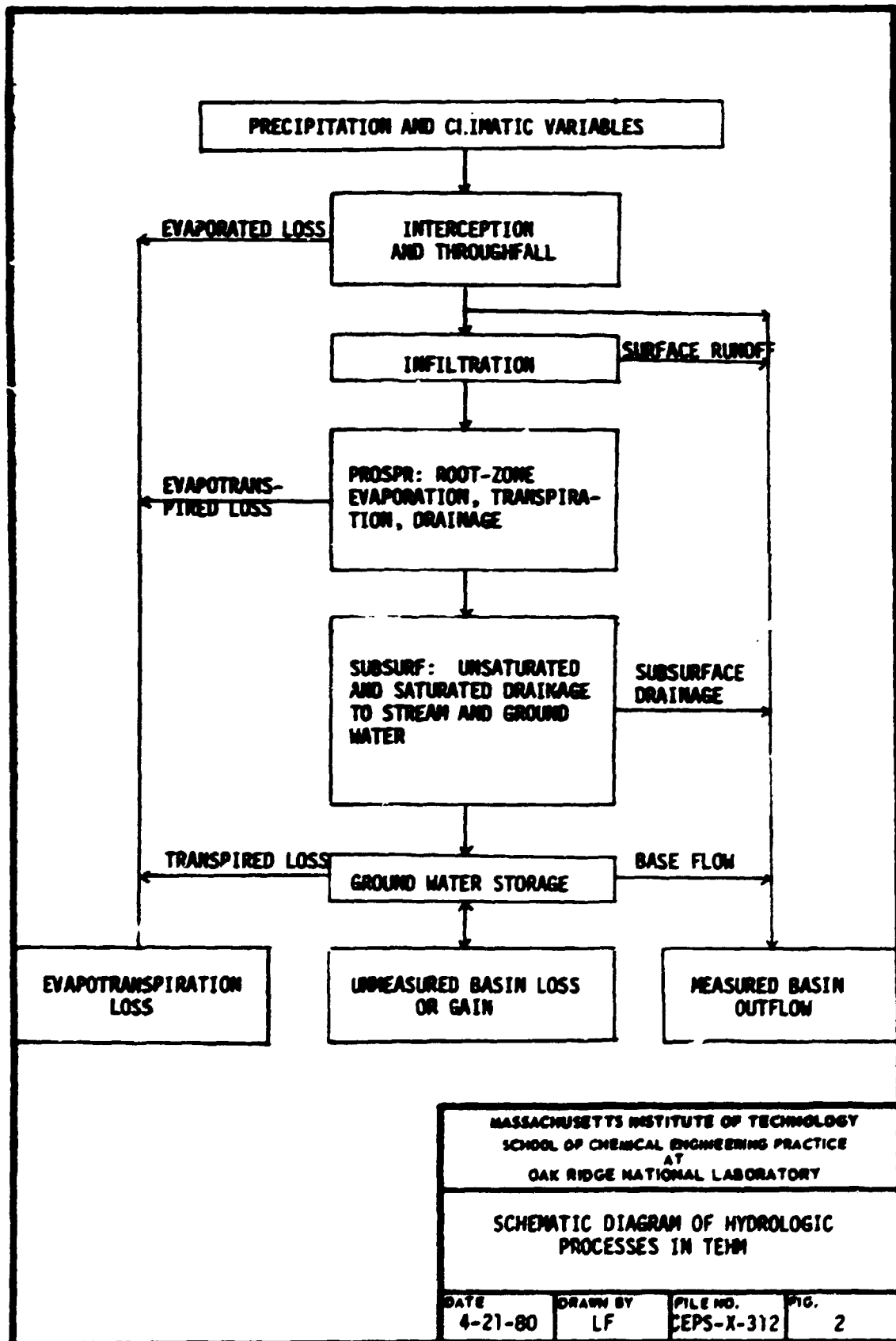
The hydraulic gradient was taken as the water potential difference from macropores to mesopores divided by half the distance between centers of two neighboring macropores.

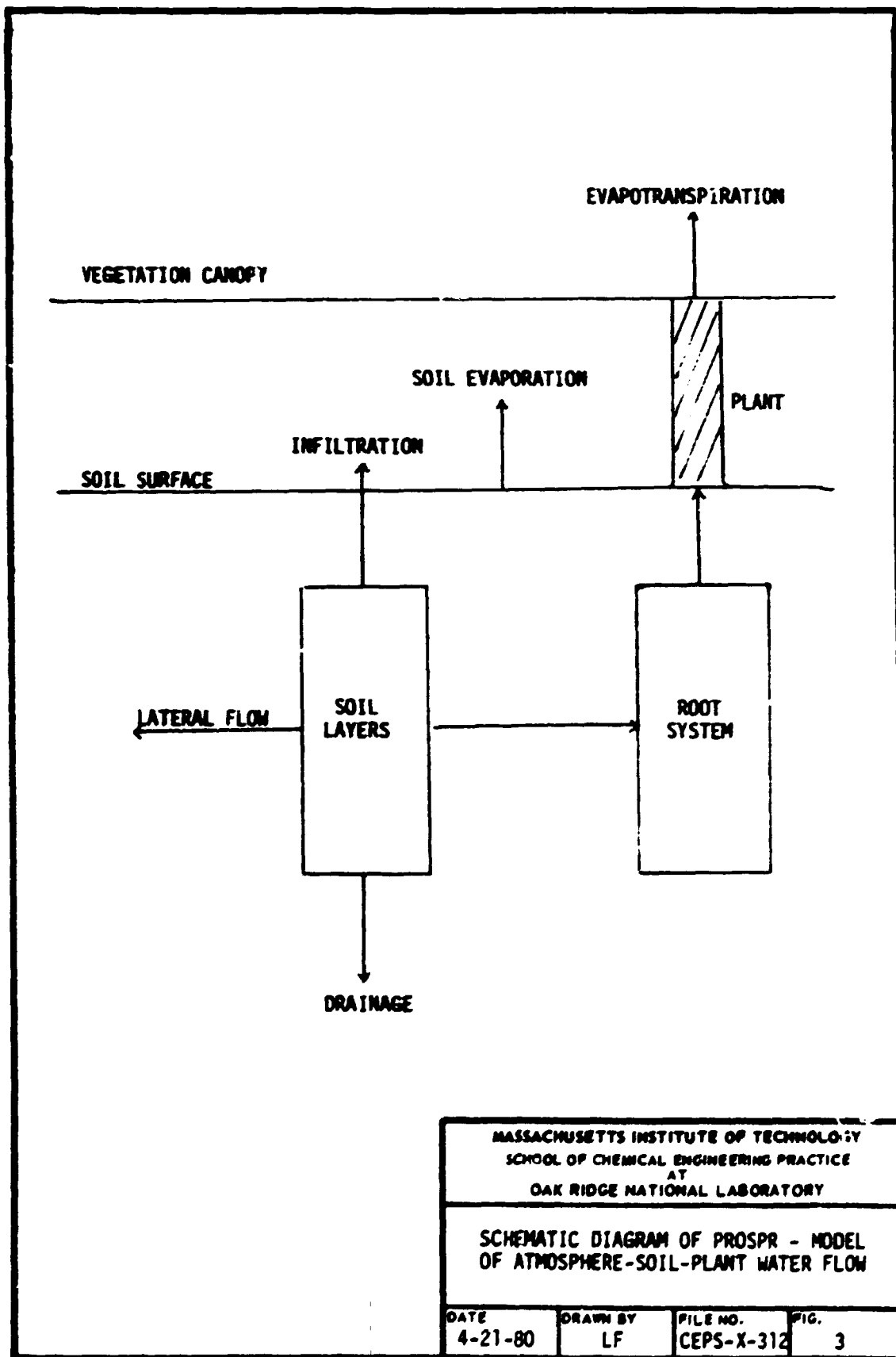
Flow between layers into macropores was accounted for whenever the mesopores of the upper layer were saturated or if water was present in the macropores of the upper layer. Flow between layers was limited by the capacity of the macropores in the lower layer. Excess from macropores was transferred to the subsequent layer, with the excess from the last layer treated as lateral flow. Therefore, excess from macropores, instead of mesopores (as in TEHM), was considered as subsurface runoff or lateral flow. In hydrologic terms this is called interflow.

4. EXISTING MODEL

The existing Terrestrial Ecosystem Hydrologic Model (TEHM) contains the subroutine for Soil-Plant Water Flow (PROSPR). TEHM is a mechanistic model of hydrologic processes in vegetated land for simulation of interception and throughfall, infiltration, evapotranspiration and drainage, and surface and subsurface flow (3). A schematic diagram of the hydrologic processes involved is shown in Fig. 2. Precipitation data, climatic variables, vegetation characteristics, and soil properties are the major inputs to the model.

PROSPR, a subroutine in TEHM, simulates soil-layer drainage and root-zone soil-plant interactions, as shown in Fig. 3. The subroutines for macropore flow effects were incorporated into the part of PROSPR for modeling water flow through soil layers. In PROSPR, precipitation infiltrates through the surface into the mesopores of the first layer. Any excess out





of the saturated mesopores is considered surface runoff in addition to that calculated by the infiltration algorithm. The remaining water drains through the layers; any excess at each layer is considered to be lateral flow, or interflow in hydrological terms. The drainage is the flow of mesopore water through the bottom layer of soil.

The interfacing of our model with PROSPR at different points in the program is shown in Fig. 4. Surface ponding was required for water to enter the macropores of the first soil layer. When water was already in the macropores or when the mesopores were saturated in any soil layers, macroporous flow was calculated for the particular layer.

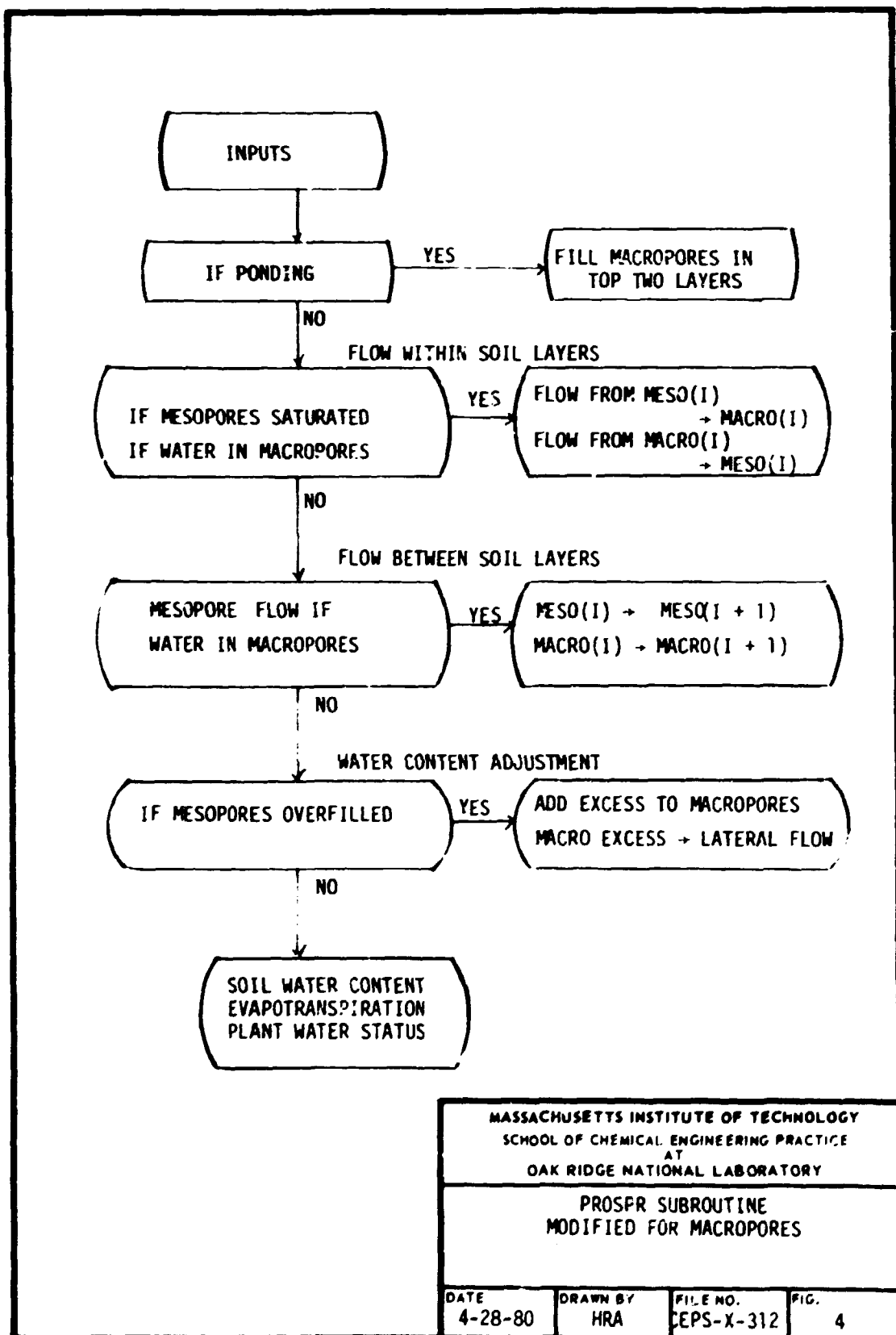
5. COMPUTER PROGRAMS

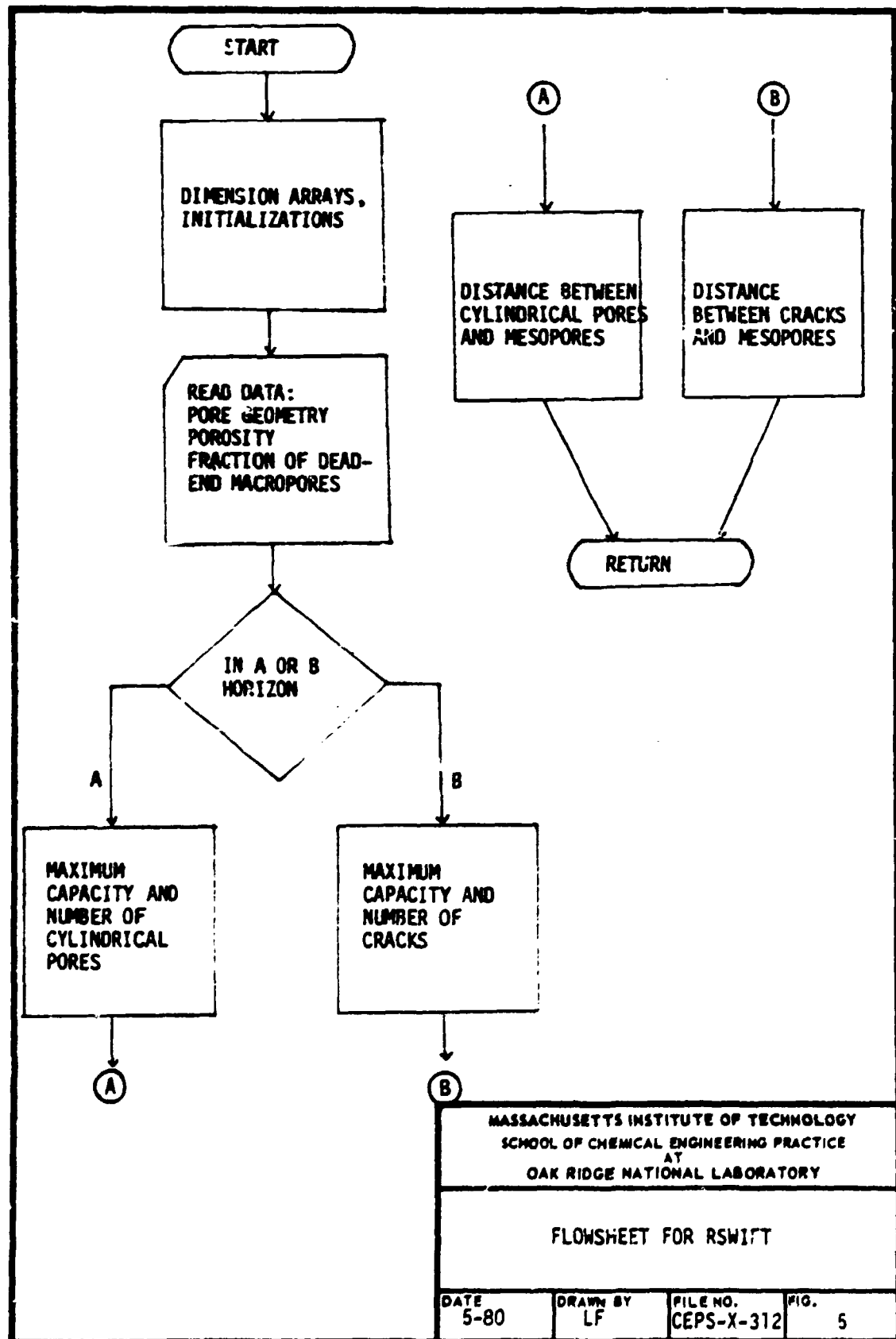
Macropore flow phenomena were simulated using inputs in the existing TEHM model and additional inputs for macroporosity, macropore geometry, and fraction of dead-end macropores. These inputs and initialization were accomplished in subroutine RSWIFT as outlined in Fig. 5. Interactive flow phenomena were developed as described in Sect. 3.4. In particular, dead-end macropores were considered as a separate but parallel case to continuous macropores, the distinction being that macropore-to-macropore flow was not allowed for dead-end macropores. When ponding existed, water was allowed to enter both continuous and dead-end macropores in the top layer. It was assumed that dead-end macropores in the top layers were open to the surface.

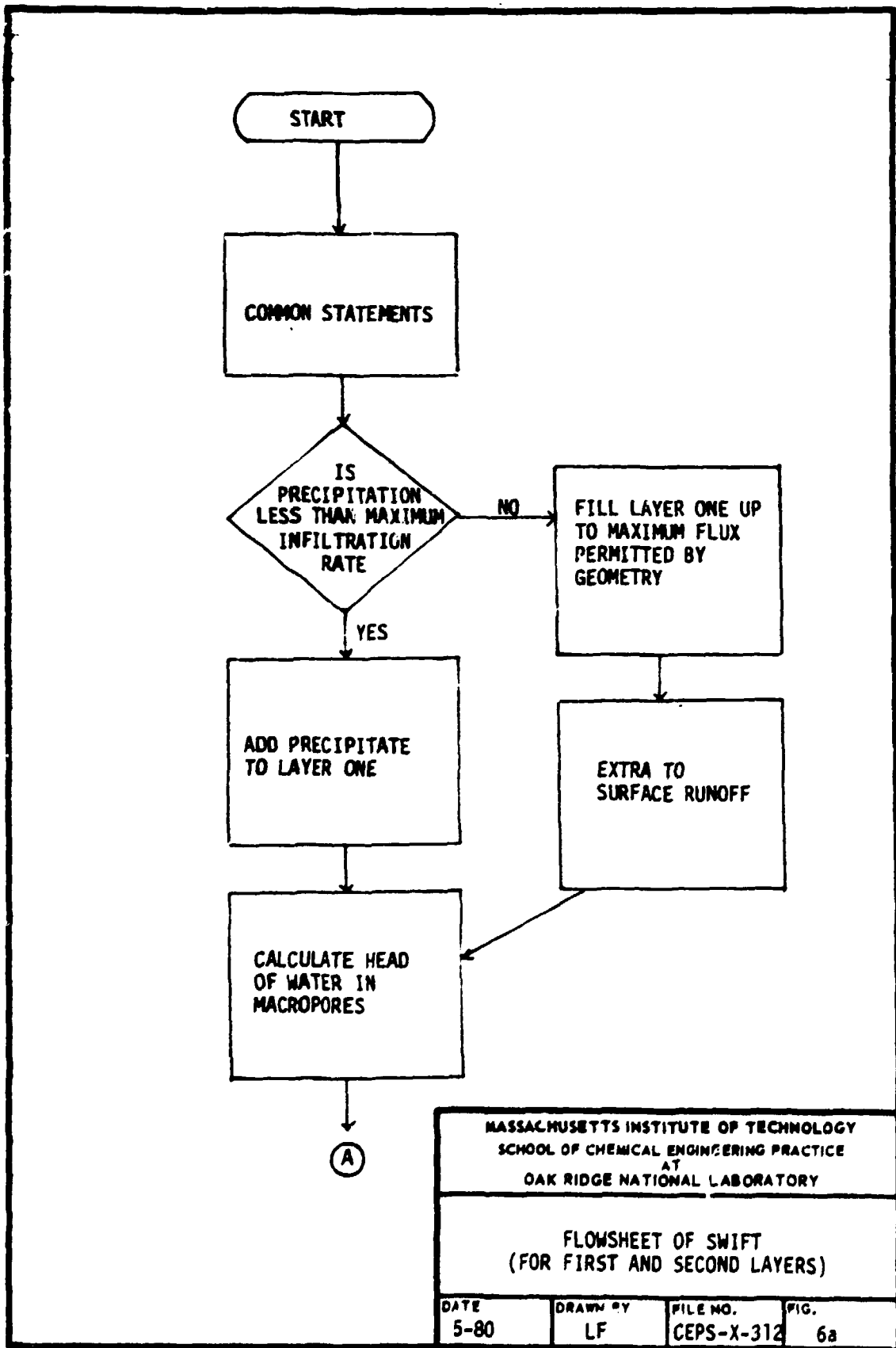
Top-layer flow effects are shown in Figs. 6a and 6b. Infiltration or macropore flow between layers was considered prior to flow between macropores and mesopores. A flow diagram of the general cases is presented in Figs. 7a and 7b. A complete daily and monthly flow history with water content data was obtained from the new model, printed from the WSWIFT subroutine. Programming details are presented in the Appendices.

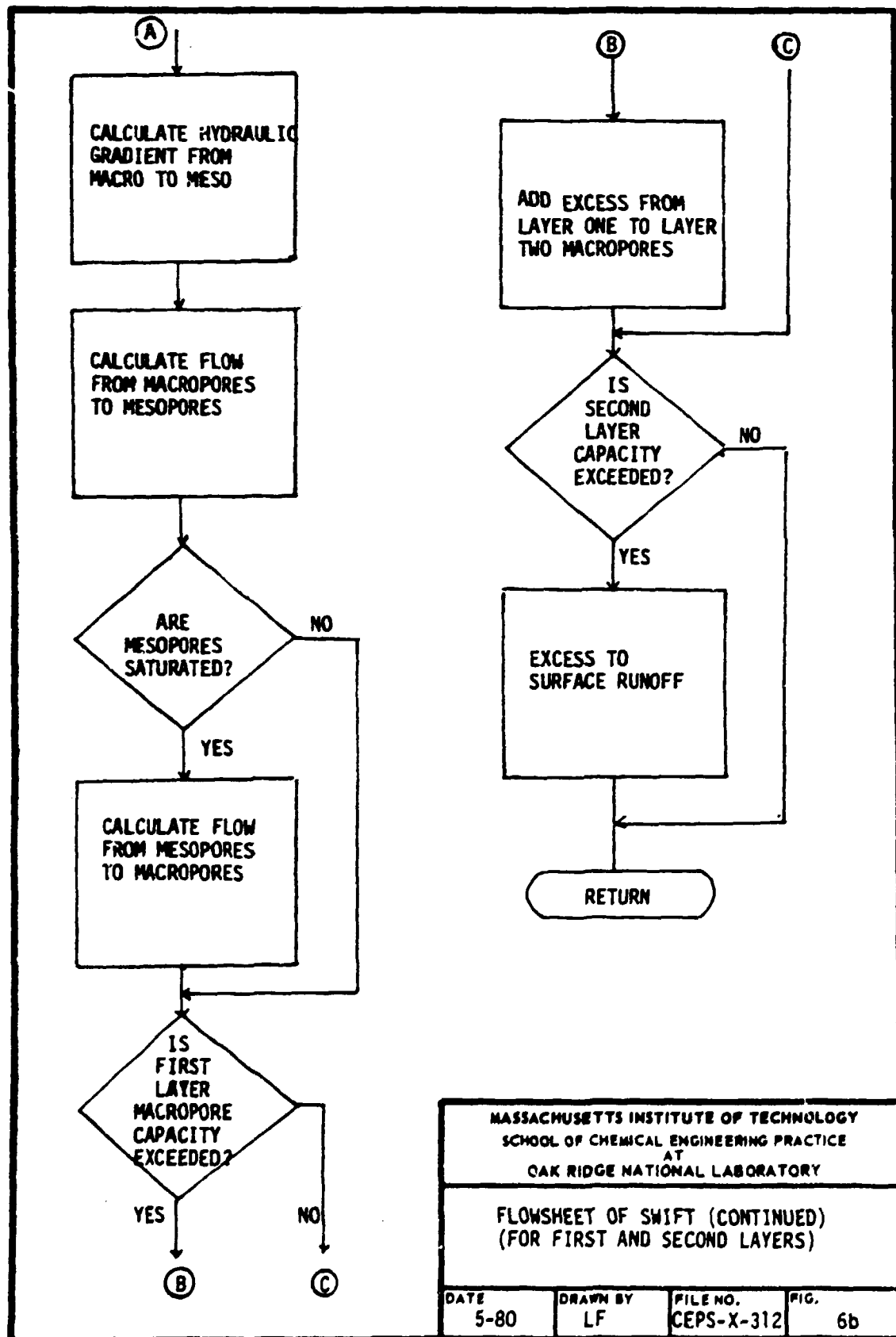
6. EVALUATION AND SENSITIVITY ANALYSIS

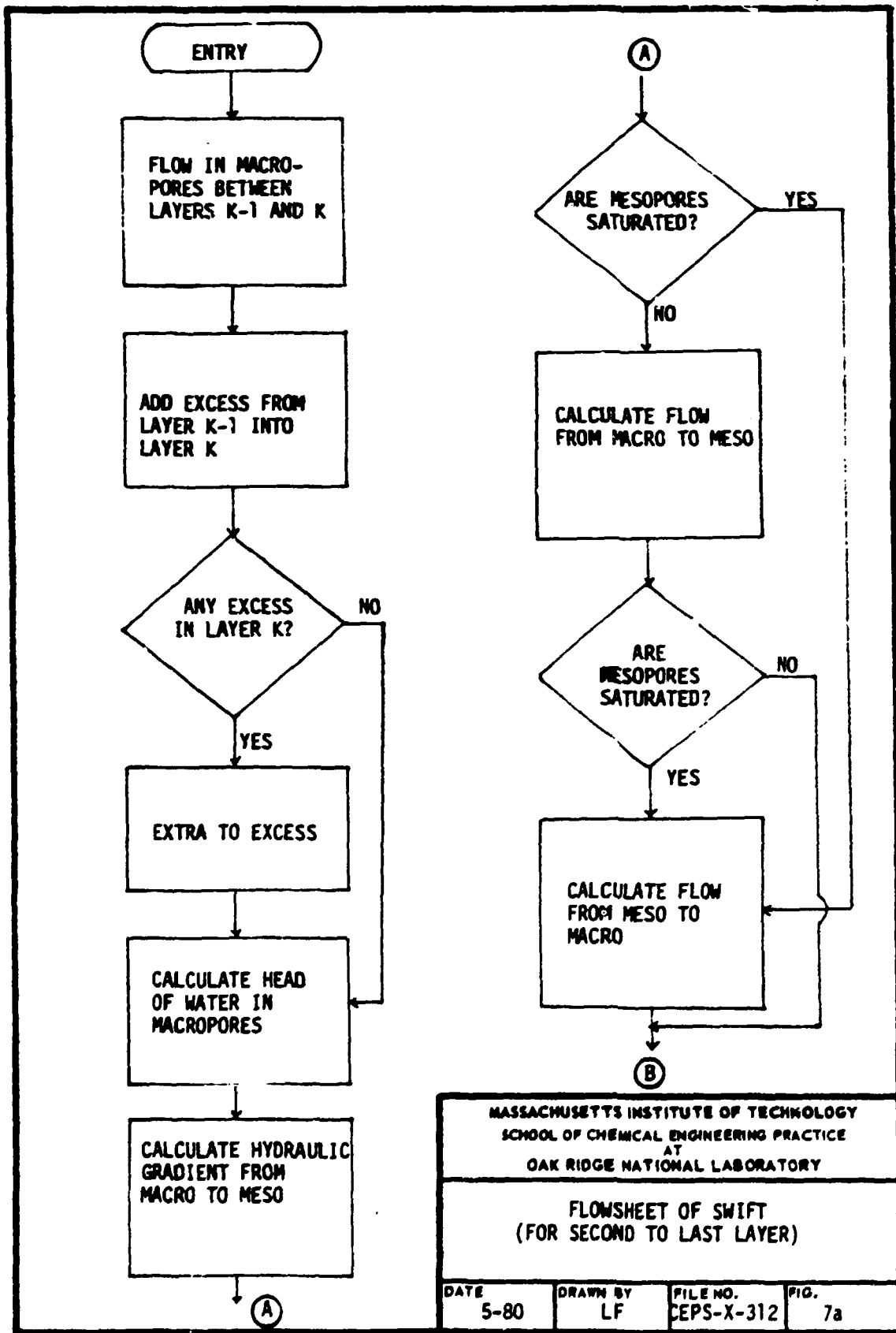
The TEHM model, with the subroutines for macropore flow effects, was analyzed parametrically with data from the Walker Branch Watershed. Meteorological data for April 1953 (close to average conditions) were used and precipitation data were adapted to test the model. Infiltration was increased tenfold for the sensitivity tests of the new subroutines. The additional inputs required in subroutine RSWIFT are described in Appendix 10.6. Sets of input data are also shown in Appendix 10.3. The program was executed for a soil profile with two layers in the A-horizon and three layers in the B-horizon. One size of pores and one configuration of pores were considered in each layer. Within each layer the macropores were assumed to have uniform geometry, porosity, and percentage of dead-end pores. Values of macroporosity were assigned to be higher in the B-horizon than in the A-horizon. This was based on observations from the field study site: macropores in the B-horizon were more numerous and continuous than those in the A-horizon.

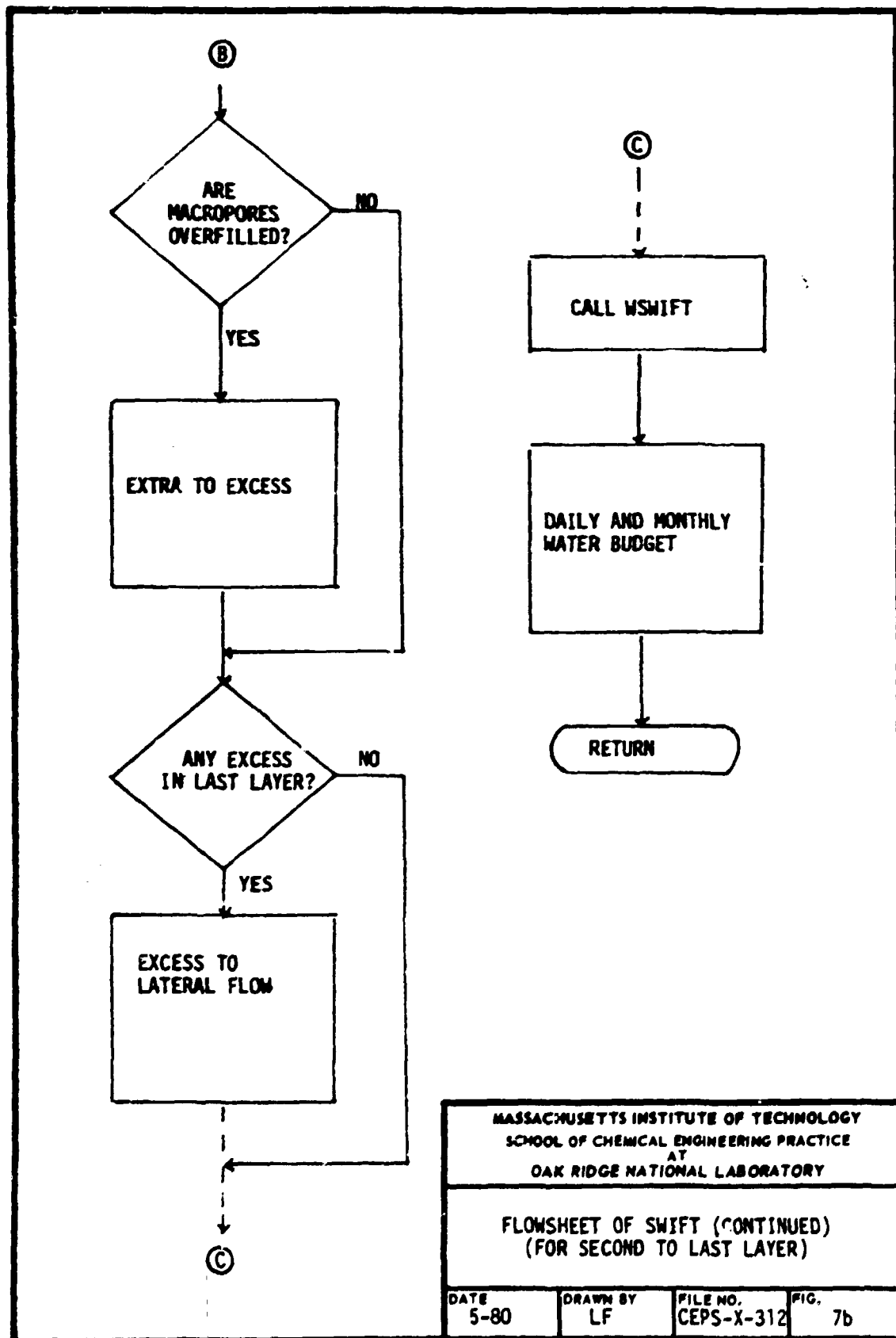












Two major runs were carried out for soils of high and low hydraulic conductivities and for varying macroporosities. Hydraulic conductivity and macroporosity are the two most important parameters for flow through macropores. The results, in the form of monthly water budgets, for soils of high and low hydraulic conductivities, are shown respectively in Figs. 8 and 9. A water budget shows:

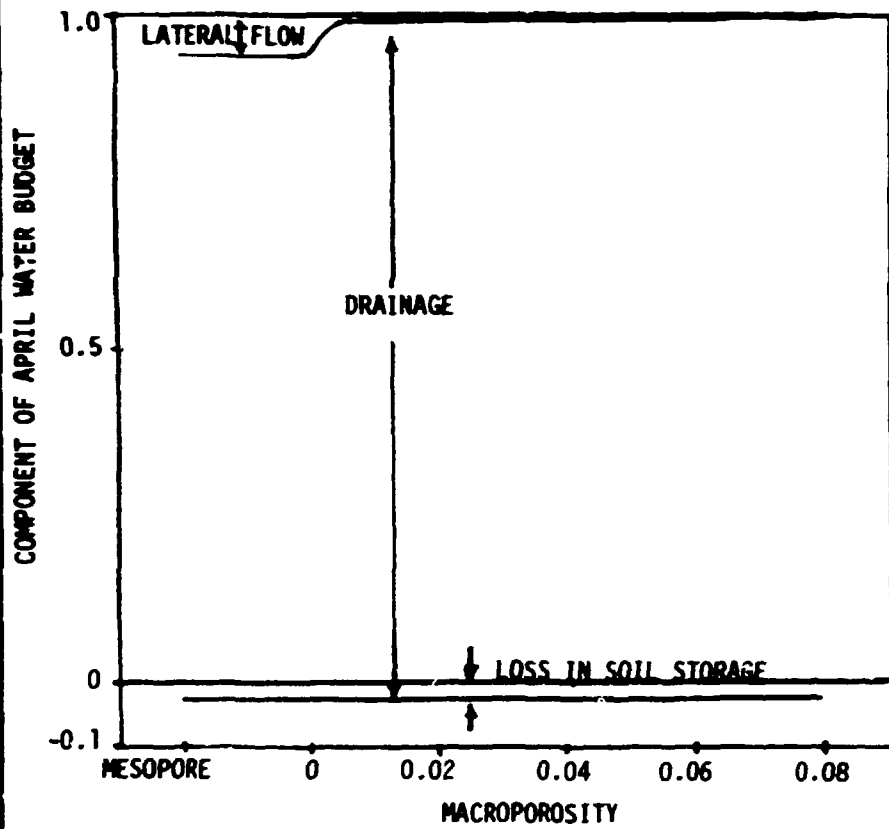
$$\text{infiltration} = \text{drainage} + \text{lateral flow} + \text{surface runoff} + \Delta \text{storage}$$

where $\Delta \text{storage}$ is the change in water content in the soil. For soil of high hydraulic conductivity, a value of 240 cm/d was used for the first layer and 120 cm/d for the subsequent layers. The different values represented the actual change in conductivity from the A-horizon, where the soil is mostly sandy, to the B-horizon, where more clay is found. The soil with lower conductivity had values of 9.6 cm/d for the first layer and 4.8 cm/d for the remaining layers. Both high and low hydraulic conductivity values are realistic and have been actually recorded for field soils. The monthly infiltration for both cases was 98 cm with no ponding. Hence, the water entered the mesopores, rather than the macropores, in the first layer.

For soil of higher hydraulic conductivity, the macropore effect was not significant, even for a macroporosity of 0.08 ml/ml (Fig. 8). Most of the water flowed through the mesopores and finally appeared in drainage. The excess, a small amount from the saturated mesopores, was transferred to the macropores. The macropores did not reach their saturation limit, and there was no lateral flow. Surface runoff was also not observed from the simulation results. A negative value was obtained for $\Delta \text{storage}$; the soil layers decreased in water content by the end of the month relative to the start of the month. On the abscissa "mesopore" indicates that subroutines for macropore effects were not called, while a macroporosity of zero represents the case where the subroutines were called but zero macroporosity was used. For both cases when the mesopores were saturated, their excess water was immediately treated as lateral flow.

In soil of low hydraulic conductivity, macropores played a much more significant role. There was a sizeable amount of both drainage and lateral flow. The drainage arose from the mesopores while the lateral flow was the excess from the macropores. The low conductivity of soil did not allow mesopores to drain water rapidly. Hence, there was a significant amount of excess from the saturated mesopores. This was transferred to the macropores, with the excess from the macropores appearing in lateral flow. Some of the water in macropores of the lower layers was transferred back to mesopores in those layers, providing a bypass around an upper saturated zone. Thus drainage from mesopores increased with increase in macroporosity for the case with low soil hydraulic conductivity (Fig. 9), and there was a corresponding decrease in lateral flow. Again, as in soil of high hydraulic conductivity, there was a loss in soil water storage. It is interesting to note the change in runoff from the case of "mesopore" to that of zero macroporosity. In the mesopore case, any excess from the first layer was

$$\text{INFILTRATION} = \text{DRAINAGE} + \text{LATERAL FLOW} + \text{RUNOFF} + \text{STORAGE}$$



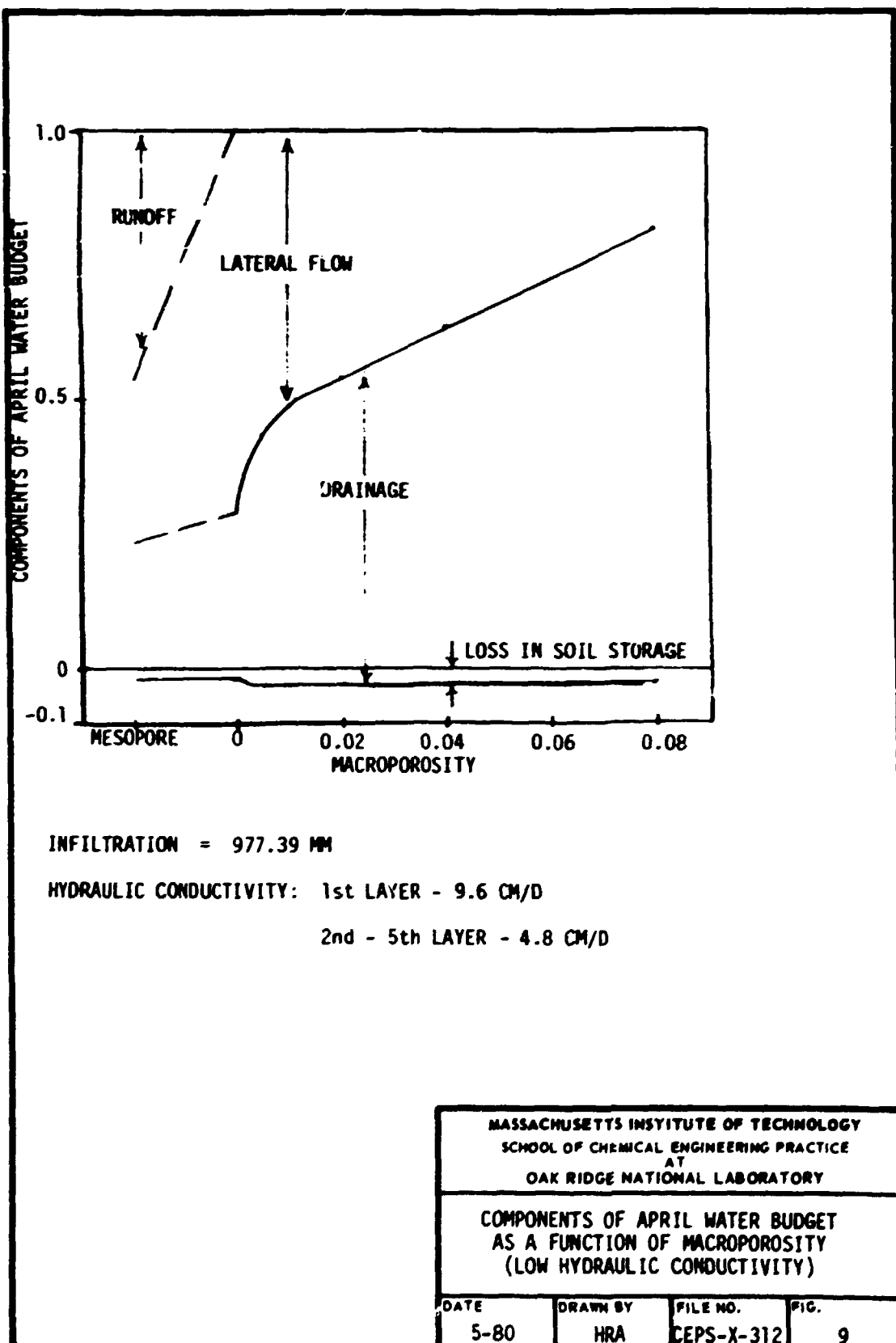
$$\text{INFILTRATION} = 977.39 \text{ MM}$$

HYDRAULIC CONDUCTIVITY: FIRST LAYER - 240 CM/D
2nd TO 5th LAYER - 120 CM/D

MASSACHUSETTS INSTITUTE OF TECHNOLOGY
SCHOOL OF CHEMICAL ENGINEERING PRACTICE
AT
OAK RIDGE NATIONAL LABORATORY

COMPONENTS OF APRIL WATER BUDGET
AS A FUNCTION OF MACROPOROSITY
(HIGH HYDRAULIC CONDUCTIVITY)

DATE 5-80	DRAWN BY HRA	FILE NO. CEPS-X-312	FIG. 8
--------------	-----------------	------------------------	-----------



sent to surface runoff. However, in the zero macroporosity case, since there was no ponding, additional runoff was not calculated. The excess was transferred to the negligible macropores and eventually to lateral flow instead.

The macropore flow effects are more clearly shown in Fig. 10. Daily flows, for a day with high infiltration (26 cm), are compared for soils of different hydraulic conductivities. The macroporosity was 0.04 ml/ml. The width of the arrows are proportional to the amount of flow. The first layer was 30-cm deep, with the subsequent layers being twice as thick. For soil of high conductivity the water was mainly transferred in mesopores, with a drainage of 25 cm and no lateral flow. On the other hand, the mesopores were quickly saturated (in the second layer) in soil of low conductivity. The excess was diverted to macropores and most of it appeared in the lateral flow (14 cm). The difference between the input and output values of the soil layers was the daily change in water content.

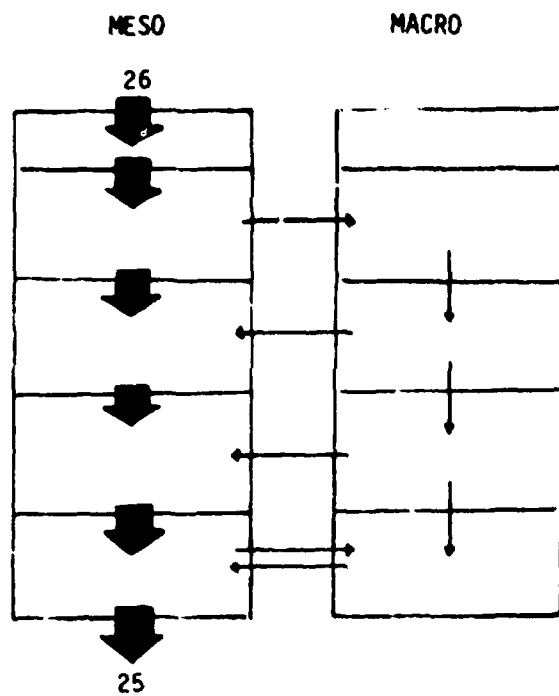
Macropore effects are more apparent when daily flows rather than monthly flows were analyzed. As macropores have significant effects during short duration, study of hourly flows are suggested.

A summary of the comparison of the two major flows, drainage and lateral flow, for soils of different hydraulic conductivity and macroporosity is shown in Table 1. Macropore effects are a strong function of hydraulic conductivity and a weaker function of macroporosity.

Table 1. Summary of Results

	<u>Drainage</u> <u>(cm/d)</u>	<u>Lateral Flow</u> <u>(cm/d)</u>
<u>Low Conductivity</u>		
Mesoporosity = 0.0	3.1	19.5
Macroporosity = 0.01	4.3	16.5
Macroporosity = 0.08	4.7	5.2
<u>High Conductivity</u>		
Mesoporosity = 0.0	23.5	1.5
Macroporosity = 0.01	24.8	0.6
Macroporosity = 0.08	25.1	0.0

$K = 240 \text{ CM/D (FIRST LAYER)}$
 $120 \text{ CM/D (OTHER LAYERS)}$



K = 9.6 CM/D (FIRST LAYER)
4.8 CM/D (OTHER LAYERS)

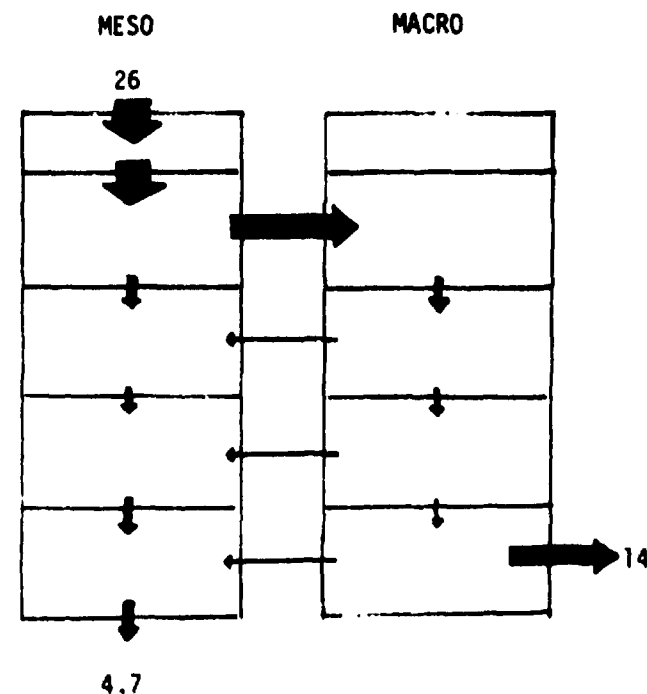


Fig. 10. MACROPORE FLOW EFFICIENCY COMPARED IN SOILS OF HIGH VS LOW CONDUCTIVITY

Infiltration and mesopore water-content profiles were also compared for heavy and light precipitation. In the absence of macropores, the water-content curve had a similar profile to the infiltration curve. Corresponding peaks were observed. With the macropore effect, most of the water drained rapidly through macropores during heavy precipitation. Thus, the peaks in the water-content curve were much reduced. This indicates that the effect of high infiltration was greatly damped in the presence of macropores. On the other hand, the macropore effect was expectedly insignificant during light precipitation.

A detailed sensitivity analysis on the other input parameters (pore shape and dimensions, percentage of dead-end pores) was not completed. However, preliminary results suggest that pore shape had an insignificant effect on drainage, whereas the proportion of dead-end macropores had a slight effect, especially on decreasing macropore-to-macropore flow and on increasing the excess water in macropores.

7. CONCLUSIONS

The presence of macropores:

1. Is important during heavy precipitation.
2. Is significant in soil of low hydraulic conductivity.
3. Increased drainage for soil of low hydraulic conductivity.
4. Decreased lateral flow for soil of low hydraulic conductivity.

8. RECOMMENDATIONS

1. The logic of subroutines SWIFT, RSWIFT, and WSWIFT should be verified.
2. A detailed sensitivity analysis should be carried out for the other input parameters: macroporosity, pore shape and dimensions, percentage of dead-end pores.
3. The importance of macropores for different soil hydraulic conductivities should be investigated, and the range of conductivity where macropores are most important should be determined. Beven and Germann concluded from their model that the presence of macropores is most significant in soil of intermediate hydraulic conductivity.
4. The programs should be tested with data from soil-block drainage study, which allows comparison with the water content profiles obtained from the soil-block facility (Fig. 13).

5. A storm analysis, which gives hourly flow information, should be carried out with our model.

9. ACKNOWLEDGMENTS

We thank R.J. Luxmoore for his extraordinary help on this project. His guidance and time were greatly appreciated. Special thanks are also given to G.T. Yeh for his interest in this work.

This research was sponsored in part by the Office of Health and Environmental Research, U.S. Dept. of Energy under contract W-7405-eng-26 with Union Carbide Corporation and in part by the Office of Toxic Substances, U.S. Environmental Protection Agency under Interagency Agreement EPA-78-D-X0387.

10. APPENDIX

10.1 Computer Logic

Three additional subroutines were used to simulate macropore phenomena. These routines executed all reading, calculating, and printing of macropore flow information. The following explanation outlines the computer calculations. Continuous and dead-end macropores were treated as separate but parallel cases so that the discussion applies to either unless otherwise stated.

Subroutine RSWIFT was called whenever a new watershed segment was simulated. All data required for the additional macropore calculations were read and initialized, then transferred to a TEHM output file. These parameters that remained constant for a soil layer were calculated. These parameters include the number and capacity of macropores, and the distance from the center of a macropore to the center of an aggregate. In addition, the number of layers in the A-horizon was calculated from the input data by assuming that only cylindrical pores were present in the A-horizon.

Water entered the mesopores unless there was ponding, in which case subroutine SWIFT was called. Precipitation entered the macropores, its rate being limited to the maximum flux, FLXMAX, permitted by the macropore geometry. Any excess from the uppermost two layers would be treated as surface runoff. It was assumed that dead-end macropores in the first layer were open to the surface. Differences in pore geometry must be considered; otherwise similar flows would be calculated for all soil layers.

In a soil layer, continuous macropore flow from the upper layer, MAFBL, was received until the capacity of the current layer was exceeded. The excess from the upper layer was then added, if possible; otherwise it would be stored in the EXCESS account and put into each subsequent layer. Excess from the last layer was considered to be lateral flow. To determine macropore-to-mesopore flow the hydraulic gradient from macropores to mesopores was calculated as the difference between mesopore water potential and the height of water (hydraulic potential) in macropores. If mesopores were saturated, they could not receive additional flow; any excess from the mesopores was transferred into the macropores. Macropore-to-mesopore flow was modeled using a Darcy-type equation:

$$\text{flow} = (\text{area of interaction})(\text{hydraulic conductivity})(\text{hydraulic gradient})$$

where flow was assumed to be mesopore-controlled by using the mesopore hydraulic conductivity. The area of interaction was the total area in a layer with water at a macropore/mesopore interface. The maximum amount of water that could flow into the mesopores was the water content of the macropores. Again, if the mesopores were overfilled, the excess was returned to the macropores. The macropores were then checked to see if they

were filled beyond capacity. Any excess was added to the EXCESS account, which was totalled daily in MACEX(K) for each soil layer (K).

The WSWIFT subroutine was called once during each simulated day. A daily and monthly summary of the flow history was produced. Daily flows between macropores and between macropores and mesopores were written and counters were reinitialized. The water contents of the mesopores and macropores were checked daily in addition to the total excess. Monthly accounts were also maintained for the flows and excess. They were initialized before further calculation in TEHM was initiated.

10.2 Computer Programs and Sample Output

Listings for subroutines SWIFT, RSWIFT, and WSWIFT follow and also a sample of the output.

10.3 Definition of Calculated Terms in Programs

Capacity of continuous macropores (cm)

$$B(K) = (\text{macroporosity})(\text{soil layer length})(\text{fraction of continuous macropores})$$

Capacity of dead end macropores (cm):

$$BD(K) = (\text{macroporosity})(\text{soil layer length})(\text{fraction of dead-end macropores})$$

Average macropore potential (cm water):

$$^{+}HWAT(K)/2 = \text{average head of water in macropores}$$

Distance from macropore to mesopores (cm):

$$\text{A-horizon: } DX(K) = \text{length of soil layer}/[(\text{total number of pores})(FRAC)(2)]$$

$$\text{FRAC} = \text{length of macropore}/\text{length of layer} = CSC(\text{angle of pore to vertical})$$

$$\text{B-horizon: } DX(K) = (2)(\text{breadth of crack} + \text{aggregate length})/6$$

Flow from macropores to mesopores (cm/time increment):

SWIFT (Main Program) Flow Calculations

LEVEL 21.2 (JUN 74)

OS/360 FORTRAN H

```

COMPILER OPTIONS - NAME= MAIN,OPT=02,LINECNT=60,SIZE=0000K,
      SOURCE,EBCDIC,ALIST,NOECK,LOAD,NAP,NOEDIT,IO,XREF

ISN 0002      SUBROUTINE SWIFT(K,DTIN)
C      THIS POLTIME ACCOUNTS FOR MACROPORE FLOW EFFECTS
ISN 0003      IMPLICIT REAL*8 (A-H,O-Z)
ISN 0004      REAL*8 MCPOR,NPOR,NAMEL,NAMEX
ISN 0005      COMMON/INPTS/MCPOR(2),PP(8),VP(8),PL(8),PERC(8),AGSIZ(8)
ISN 0006      COMMON/BITS/B(8),HWAT(8),FLOW(8),NPOR(8),DX(8)
ISN 0007      I,DFLOW(8),DHWAT(8),BD(8),JATCB
ISN 0008      COMMON/BOOKS/DMENA(8),DMAME(8),NAMEX(8),BETA(8),DBET(8)
ISN 0009      COMMON/GEOMET/DL(8),AT(2),ARAT(2),FC(8),THETA(8),SWT(8)
ISN 0010      COMMON/GEOMC/FP(8),S(8),SEV,ETGN,DMFAC,WFL,WPZ,NSL,NBL,NS
ISN 0011      COMMON/CHMOS/SURFL(8),CHETA(8),SURF1,SURF2,RLAT(8)
ISN 0012      COMMON/FIESTS/TPUNO,ZS(8),PPE,POND,TBET(8),YESMAC,PSM(8)
ISN 0013      DATA TNCPI/6.28318531/,EXCESS/0.0/,FLXMAX/0.0/
ISN 0014      DATA BYFS/-5/,FRAC/1.414213562/
C      ESTIMATIVE STEP IN FRACTIONAL DAYS
C      DATA, AS IN PROSPR, ARE PER C4**2
C
C      FIRST LAYER MACROPORES
C      SURFACE INFILTRATION AND RUNOFF ACCOUNTED FOR
ISN 0015      RAIN=PRE
ISN 0016      FLXMAX=MAX INFILTRATION RATE (CM/TIME STEP)
ISN 0017      FLXMAX=12250.*RP(1)*92*NCPCR(1)*86400.*DTIN
ISN 0018      IF(POND.EQ.0.0)RAIN=0.0
ISN 0019      IF FLXMAX EXCEEDED ALLOW RUNOFF
ISN 0020      IF(PAIN.LE.FLXMAX)GO TO 250
ISN 0021      C ASSUME ALL DEAD END MACROPORES IN FIRST LAYER OPEN TO SURFACE
ISN 0022      DMENA=DMENA(1)+FLXMAX*(1.-PERC(1))
ISN 0023      DBET(1)=DBET(1)+FLXMAX*PERC(1)
ISN 0024      TRUNO=TRUNO+RAIN-FLXMAX
ISN 0025      GO TO 300
ISN 0026      250  DBET(1)=DBET(1)+RAIN*PERC(1)
ISN 0027      BETA(1)=BETA(1)+RAIN*(1.-PERC(1))
ISN 0028      300  HWAT(1)=BETA(1)/(NCPCP(1)*(1.-PERC(1)))
ISN 0029      DMGRAD1=(PSM(1)+HWAT(1)/2.)/(FP(1)+DLOG(DX(1)/RP(1)))
ISN 0030      DMGRAD=(PSM(1)+DMGRAD1)/2.)/(RP(1)+DLOG(DX(1)/RP(1)))
ISN 0031      DMENA KEEPS TRACK OF DAILY MESO TO MACROPORE FLOW
ISN 0032      IF(THETA(1).LE.S(1))GO TO 302
ISN 0033      DMENA(1)=DMENA(1)+(THETA(1)-S(1))
ISN 0034      FLOW(1)=0.0
ISN 0035      DFLOR(1)=0.0
ISN 0036      GO TO 305
ISN 0037      C CALCULATE MACROPORE TO MESOPORE FLOW
ISN 0038      FLOW(1)=TBOP1*RP(1)*FRAC*HWAT(1)*ZS(1)*DT1*DMGRAD1*NPOR(1)
ISN 0039      *(1.-PERC(1))
ISN 0040      DFLOR(1)=TBOP1*RP(1)*FRAC*HWAT(1)*ZS(1)*DT1*DMGRAD*NPOR(1)
ISN 0041      *(1.-PERC(1))
ISN 0042      IF(FLOW(1).GT.BETA(1))FLOW(1)=BETA(1)
ISN 0043      IF(DFLOR(1).GT.DBET(1))DFLOR(1)=DBET(1)
ISN 0044      C DMENA KEEPS TRACK OF DAILY MACRO TO MESOPORE FLOW
ISN 0045      DMENA(1)=DMENA(1)+FLCW(1)+DFLOR(1)
ISN 0046      THETA(1)=THETA(1)+FLCW(1)+DFLOR(1)
ISN 0047      BETA(1)=BETA(1)-FLOW(1)
ISN 0048      DBET(1)=DBET(1)-DFLOR(1)
ISN 0049      IF(THETA(1).LE.S(1))GO TO 310
ISN 0050      DMENA(1)=DMENA(1)-(THETA(1)-S(1))

```

SWIFT (continued)

```

      C      FLOW FROM MESOPORE TO MACROPCRE
  ISN 0046  305  BETA(1)=BETA(1)+(THETA(1)-S(1))*(1.-PERC(1))
  ISN 0050  DBET(1)=DBET(1)+(THETA(1)-S(1))*PERC(1)
  ISN 0051  THETA(1)=S(1)
  ISN 0052  310  CONTINUE
  ISN 0053  IF(BETA(1).LE.B(1))GC TO 315
      C      IF EXCEED CAPACITY ADD TO SECOND LAYER
  ISN 0055  BETA(2)=BETA(2)+BETA(1)-E(1)
  ISN 0056  DMAMA(2)=DMAMA(2)+(BETA(1)-B(1))
  ISN 0057  BETA(1)=B(1)
  ISN 0058  315  IF(DBET(1).LE.RD(1))GC TO 320
      C      IF EXCEED CAPACITY ALLOC RUNOFF
  ISN 0060  TRUNO=TRUNO+DBET(1)-ED(1)
  ISN 0061  DRET(1)=BD(1)
  ISN 0062  320  IF(BETA(2).LE.B(2))GC TO 350
  ISN 0064  TRUNO=TRUNO+BETA(2)-E(2)
  ISN 0065  BETA(2)=B(2)
  ISN 0066  350  EXCESS=0.0
  ISN 0067  TBET(1)=BETA(1)+DRET(1)
  ISN 0068  RETURN
  ISN 0069  ENTPY SLBONE(K,DTW)

      C      MACROPORE FLOW BETWEEN LAYERS (K-1) AND (K)
  ISN 0070  MAFBL=BETA(K-1)
  ISN 0071  IF(MAFBL.LE.(B(K)-BETA(K)))GC TO 370
  ISN 0072  MAFBL=B(K)-BETA(K)
  ISN 0073  BETA(K-1)=BETA(K-1)-MAFBL
  ISN 0074  BETA(K)=B(K)
  ISN 0075  GO TO 360
  ISN 0076  360  BETA(K)=BETA(K)+MAFBL
  ISN 0077  BETA(K-1)=0.0
  ISN 0078  ISN 0079  380  CONTINUE
  ISN 0080  DMAMA(K)=DMAMA(K)+MAFBL
      C      ACCOUNTING FOR FLOW WITHIN LAYERS
      C      FLOW(K)=FLOW FROM MACROPORES TO MESOPORES
  ISN 0081  BETA(K)=BETA(K)+EXCESS
  ISN 0082  EXCESS=0.0
  ISN 0083  IF(BETA(K).LE.B(K))GC TO 400
  ISN 0084  EXCESS=BETA(K)-B(K)
  ISN 0085  BETA(K)=B(K)
  ISN 0086  400  HWAT(K)=BETA(K)/(MCPOR(K)*(1.-PERC(K)))
  ISN 0087  -HWAT(K)=DBET(K)/(MCPOR(K)*PERC(K))
  ISN 0088  DHGRAD=(PSW(K)+HWAT(K)/2.)/CX(K)
  ISN 0089  HGRAD=(PSW(K)+HWAT(K)/2.)/CX(K)
  ISN 0090  IF(THETA(K).LE.S(K))GC TO 450
  ISN 0091  FLOW(K)=0.0
  ISN 0092  OFLOW(K)=0.0
  ISN 0093  DMENA(K)=DMENA(K)+(THETA(K)-S(K))
  ISN 0094  GO TO 570
  ISN 0095  450  IF(K.GT.IATOB) GO TO 500
  ISN 0096  DBGRAD=(PSW(K)+HWAT(K)/2.)/(RP(K)*DLCG(DX(K)/RP(K)))
  ISN 0097  -HGRAD=(PSW(K)+HWAT(K)/2.)/(RP(K)*DLCG(DX(K)/RP(K)))
  ISN 0098  500  FLOW FROM MACROPORE CYLINDERS
  ISN 0099  FLOW(K)=TWCPI*RP(K)*FRAC*HWAT(K)*ZS(K)*DTIN*HGRAD*NPOR(K)*
  ISN 0100  1*(1.-PERC(K))
  ISN 0101  OFLOW(K)=TWCPI*RP(K)*FRAC*HWAT(K)*ZS(K)*DTIN*HGRAD*NPOR(K)*
  ISN 0102  1*PERC(K)
  ISN 0103  GO TO 550

```

SHIFT (continued)

```

ISN 0104      50C   X=BYP5*4GSIZE(K)
C               FLOW FRCN MACROPORE CRACKS
ISN 0105      FLOW(K)=2.0*(WP(K)+PL(K))*(X*FRAC+(1.-X))
ISN 0106      1.0HWAT(K)=ZS(K)*DT*W*HGRAD*NPER(K)*(1.-PERC(K))
DPL0V(K)=2.0*(WP(K)+PL(K))*(X*FRAC+(1.-X))*NPER(K)*PERC(K)
1.0DHWAT(K)=ZS(K)*DT*N*HGRAD
ISN 0107      550   IF(FLOW(K).GT.*BETA(K))FLOW(K)=BETA(K)
ISN 0108      IF(DPL0V(K).GT.*DBET(K))DPL0V(K)=DBET(K)
ISN 0111      DNAME(K)=DNAME(K)+FLCN(K)+DPL0V(K)
ISN 0112      THETA(K)=THETA(K)+FLC4(K)+DPL0V(K)
ISN 0113      IF(THETA(K).LT.0.0) CALL ERROR
ISN 0114      BETA(K)=BETA(K)-FLOW(K)
ISN 0116      DBET(K)=DBET(K)-DPL0V(K)
ISN 0117      IF(THETA(K).LE.S(K)) GO TO 590
ISN 0119      DNAME(K)=DNAME(K)-(THETA(K)-S(K))
C               FLOW FRCN Meso TO MACROPORE (IF MESOPORES OVERFILLED)
ISN 0120      570   BETA(K)=BETA(K)+(THETA(K)-S(K))*(1.-PERC(K))
ISN 0121      DBET(K)=DBET(K)+(THETA(K)-S(K))*PERC(K)
C               WRITE(6,707)THETA(K),BETA(K),DBET(K),K
C707      FORMAT(' SWFT121 ',3G16.5,13)
ISN 0122      THETA(K)=S(K)
ISN 0123      IF(DBET(K).LE.BD(K))GO TO 580
ISN 0125      EXCESS=EXCESS+DBET(K)-BD(K)
C               WRITE(6,750)EXCESS,DBET(K),BD(K),K
C750      FORMAT(' SWFT122 ',3G16.5,13)
ISN 0126      DBET(K)=BD(K)
ISN 0127      580   CONTINUE
ISN 0128      IF(BETA(K).LE.B(K))GO TO 590
ISN 0130      EXCESS=EXCESS+BETA(K)-B(K)
C               WRITE(6,775)EXCESS,BETA(K),B(K),K
C775      FORMAT(' SWFT134 ',3G16.5,13)
ISN 0131      BETA(K)=B(K)
C               BETA(NSL) ENTERS MESCOPORES
ISN 0132      59C   MACEX(K)=MACEX(K)+EXCESS
C               IF(MACEX(K).GT.0.0) WRITE(6,777) K,MACEX(K),EXCESS,EETA(K),DBET(K)
C               1,THETA(K),FLOW(K),DPL0V(K),DNAME(K),DNAME(K),
C               2,RLAT(K),TRUND,FLXMAX
C777      FORMAT(' ',1I,13D10.3)
ISN 0133      IF(MACEX(K).GT.100.) CALL ERROR
ISN 0135      IF(K.NE.NSL)GO TO 600
ISN 0137      RLAT(K)=RLAT(K)+EXCESS
ISN 0138      EXCESS=C.0
ISN 0136      600   TBET(K)=BETA(K)+DBET(K)+EXCESS
ISN 0140      RETURN
ISN 0141      END

```

RSWIFT (Read Data, Initializations)

LEVEL 21.8 (JUN 74)

OS/360 FORTRAN H

```

COMPILER OPTIONS - NAME= MAIN,CPT=02,LINECNT=60,SIZE=0000K.
SOURCE=EBCDIC,NCLIST=NONECK,LCAP=MAP,NOEDIT,IO,XREF

ISN 0002      SUBROUTINE RSWIFT
C THIS ROUTINE READS AND INITIALIZES FOR SWIFT
C SWIFT POUTINE ACCOUNTS FOR MACROPORE FLOW EFFECTS
IMPLICIT REAL*8 (A-H,O-Z)
REAL*8 MCPOR,NPOR,NFBL,NACEX,NNACEX,NNENE
NNENE
COMMON/INPTS/ MCPOR(8),RP(8),WP(8),PL(8),PERC(8),AGSIZE(8)
COMMON/EITS/ B(8),HWAT(8),FLCW(8),NPOR(8),DX(8)
DX(8)
COMMON/BOOKS/DMENE(8),DMANA(8),NACEX(8),BETA(8),DBET(8)
COMMON/GEOMET/DL(8),AT(2),ARAT(2),FC(8),THETA(8),SUT(8)
COMMON/FORCES/VP(8),F,S(8),SEV,ETGW,DNFAC,WF1,WF2,NSL,NBL,NS
COMMON/CHMOS/SWFBL(8),CHETA(8),SWRF1,SWRF2,PLAT(8)
COMMON/PIECES/TRUNO,ZS(8),PRE,POND,TBET(8),YESMAC,PSM(8)
COMMON/PONTHS/NNENE(2),NNENE(8),NNANA(8),NNACEX(8),NNENE(8)
COMMON/RESOP/DMENE(2)

ISN 0008      C VARIABLES IN COMMONS BOOKS & MONTHS DEFINED IN RSWIFT
DATA PI/3.14159265358979/
DATA FRAC/1.414213562/
C DATA INPUTS
C VALUES ARE FOR A 1-CM*#2 CROSS SECTION
C FRAC=COSEC(ANGLE OF A PORE TO THE VERTICAL)
C I REFERS TO A SOIL LAYER
C MCPOR(I)=TOTAL MACROPORESTY (ML/ML)
C RP(I)=RADIUS OF CYLINDRICAL PORE (CM)
C WP(I)=DEPTH OF RECTANGULAR CRACK (CM)
C PL(I)=DEPTH OF RECTANGULAR CRACK (CM)
C AGSIZE(I)=AVG LENGTH OF AGGREGATE (CM)
C PERC(I)=FRACTION OF MACROPORES WHICH ARE DEAD END
C BETA(I)=WATER CONTENT OF CONTINUOUS MACROPORES (CM/LAYER)
C S(I)=MAX CAPACITY OF CONTINUOUS MACROPORES (SATURATED CM/LAYER)
C DBET(I)=WATER CONTENT OF DEAD END MACROPORES (CM/LAYER)
C BD(I)=MAX CAPACITY OF DEAD END MACROPORES (CM/LAYER)
C HWAT(I)=HEAD OF WATER IN CONT. MACROPORES (CM OF WATER)
C DHWAT(I)=HEAD OF WATER IN DEAD END MACROPORES (CM OF WATER)
C NPOR(I)=TOTAL NUMBER OF MACROPORES (#/LAYER)
C TBET(I)=TOTAL WATER CONTENT OF MACROPORES (CM/LAYER)
C DX(I)=DISTANCE FROM MACROPORES TO MESOPORES (CM)
C FOLLOWING VARIABLES ORIGINATE IN PROSPR
C DL(I)=DEPTH OF SOIL LAYER (CM)
C THETA(I)=WATER CONTENT OF MESOPORES (CM/LAYER)
C S(I)=MAX CAPACITY OF MESOPORES (CM/LAYER)
C NSL=NUMBER OF SOIL LAYERS
C PLAT(I)=LATERAL FLOW (CM/TIME STEP)
C TRUNO=SURFACE RUNOFF (CM/TIME STEP)
C ZS(I)=HYDRAULIC CONDUCTIVITY (CM/DAY)
C DTIM=TIME STEP (FRACTIONAL DAYS)
C PRE=PRECIPITATION (CM/TIME STEP)
C POND=SWITCH SET TO 1 IF THERE IS SURFACE PONDING
C YESMAC=SWITCH SET TO 0 IF NEGLECTING MACROPORES
C PSM(I)=HYDRAULIC POTENTIAL IN MESOPORES (CM OF WATER)
C IATOB=NUMBER OF SOIL LAYERS IN A HORIZON
C NOMINAL VALUES ARE USED FOR ZERO INPUT DATA OF MCPOR,RP,WP,
C PL,PERC AND AGSIZE
C IATOB=0
C POND=0.
ISN 0017
ISN 0018

```

RSWIFT (continued)

```

ISM 0019      WRITE(6,100)
ISM 0020      100  FORMAT(' LEVEL POROSITY  FCPE RADIUS  WIDTH  LENGTH
ISM 0021          1PERCENTAGE  AGSIZE ')
ISM 0022          DO 170 I=1,NSL
ISM 0023          READ(5,150)NCPOR(I),LP(I),VP(I),PL(I),PERC(I),AGSIZE(I)
ISM 0024          150  FORMAT(6F10.4)
ISM 0025          C      IATOB=NUMBER OF LAYERS IN "A" HORIZON
ISM 0026          IF(PL(I).LE.1.00-10) IATCP=IATOB+1
ISM 0027          C      SET NOMINAL VALUES FOR ZERO INPUT DATA
ISM 0028          IF (PCPCR(I).EQ.0.0) VCPGR(I)=1.0-12
ISM 0029          IF (RP(I).EQ.0.0) RP(I)=1.0-12
ISM 0030          IF (VP(I).EQ.0.0) VP(I)=1.0-12
ISM 0031          IF (PL(I).EQ.0.0) PL(I)=1.0-12
ISM 0032          IF (PERC(I).EQ.0.0) PERC(I)=1.0-12
ISM 0033          IF (AGSIZE(I).EQ.0.0) AGSIZE(I)=1.0-12
ISM 0034          WRITE(6,160)NCPOR(I),RP(I),VP(I),PL(I),PERC(I),AGSIZE(I)
ISM 0035          160  FORMAT(2X,12,2X,6F10.4)
ISM 0036          170  CONTINUE
ISM 0037          DO 200 I=1,NSL
ISM 0038          C      INITIALIZING WATER BUDGET ACCOUNTS
ISM 0039          BETA(I)=0.0
ISM 0040          DOET(I)=0.0
ISM 0041          TBET(I)=0.0
ISM 0042          DMENE(I)=0.0
ISM 0043          DMENA(I)=0.0
ISM 0044          DNAME(I)=0.0
ISM 0045          DRAMA(I)=0.0
ISM 0046          MAEX(I)=0.0
ISM 0047          MMENE(I)=0.0
ISM 0048          MMENA(I)=0.0
ISM 0049          MMAME(I)=0.0
ISM 0050          MMACE(I)=0.0
ISM 0051          B(I)=NCPOR(I)*DL(I)*(1.-PERC(I))
ISM 0052          SD(I)=NCPOR(I)*DL(I)*PERC(I)
ISM 0053          IF(I.GT.IATOB)GO TO 190
ISM 0054          C      NO. OF CYLINDERS IN "A" HORIZON LAYER
ISM 0055          NPOP(I)=NCPOR(I)/(D(RP(I)*2.*FRAC))
ISM 0056          C      ASSUMES MACROPORE LENGTH=FRAC*DL(I)
ISM 0057          DX(I)=DL(I)/(NPOP(I)*2.*FRAC)
ISM 0058          GO TO 200
ISM 0059          C      NO. OF CRACKS IN "B" HORIZON LAYER
ISM 0060          NPOP(I)=NCPOR(I)*DL(I)/(VP(I)*PL(I)*AGSIZE(I))
ISM 0061          DX(I)=(2.*PL(I)+AGSIZE(I))/6.
ISM 0062          190  CONTINUE
ISM 0063          RETURN
ISM 0064          200
ISM 0065          ENO
ISM 0066

```

WSWIFT (Write Results)

LEVEL 21.E (JUN 74)

CS/360 FORTRAN H

```

COMPILER OPTIONS - NAME= MAIN,CPT=02,LINECNT=60,SIZE=0000K,
SOURCE,EBCDIC,NOLIST,NOECK,LCAO,NAP,NOEDIT,ED,XREF

ISN 0002      SUBROUTINE WSWIFT
ISN 0003      C ROUTINE TO PRINT OUT DAILY/MONTHLY WATER STATUS
ISN 0004      IMPLICIT REAL*8 (A-H,O-Z)
ISN 0005      REAL*8 DMEXX,MMEXA,MMAME,MMAPA,MMACEX,MMENE
ISN 0006      DIMENSION DBETA(8),DBET(8),DTET(8)
ISN 0007      COMMON/MONTHS/MMAME(8),MMENA(8),MMAMA(8),MMACEX(8),MMENE(8)
ISN 0008      COMMON/MESOP/DMAME(8)
ISN 0009      COMMON/GEOMT/DL(8),AT(2),ARAT(2),PC(8),THETA(8),SNT(8)
ISN 0010      COMMON/PORES/VP(8),P,S(8),SEV,ETGV,DPAC,WF1,WP2,NSL,NEL,NS
ISN 0011      COMMON/EDOKS/DMENA(8),DMAME(8),DMANA(8),MACE(8),BETA(2),DBET(8)
ISN 0012      DMAME(J)=DAILY MESOPORE TO MACROPORE FLOW
ISN 0013      DMENE(J)=DAILY MESOPORE TO MESOPORE FLOW
ISN 0014      DMAME(J)=DAILY MACROPORE TO MESOPORE FLOW
ISN 0015      DMANA(J)=DAILY MACROPORE TO MACROPORE FLOW
ISN 0016      MACE(X)(J)=DAILY MACROPORE EXCESS
ISN 0017      MMAME(J)=MONTHLY MACROPORE TO MESOPORE FLOW
ISN 0018      MMENA(J)=MONTHLY MESOPORE TO MACROPORE FLOW
ISN 0019      MMENE(J)=MONTHLY MESOPORE TO MESOPORE FLOW
ISN 0020      MMAMA(J)=MONTHLY MACROPORE TO MACROPORE FLOW
ISN 0021      MMACEX(J)=MONTHLY MACROPORE EXCESS
ISN 0022      DO 111 J=1,NSL
ISN 0023      DBETA(J)=BETA(J)/DL(J)
ISN 0024      DBET(J)=DBET(J)/DL(J)
ISN 0025      DTET(J)=THETA(J)/DL(J)
ISN 0026      C DAILY WATER STATUS
ISN 0027      111 CONTINUE
ISN 0028      WRITE(6,130)(DMAME(I),I=1,NSL)
ISN 0029      100 FORMAT(' DMAME (CM/DAY) ',8(E12.4,2X))
ISN 0030      WRITE(6,200)(MMAME(I),I=1,NSL)
ISN 0031      200 FORMAT(' MMAME (CM/DAY) ',8(E12.4,2X))
ISN 0032      WRITE(6,300)(MMENA(I),I=1,NSL)
ISN 0033      300 FORMAT(' MMENA (CM/DAY) ',8(E12.4,2X))
ISN 0034      WRITE(6,400)(MACE(X),I=1,NSL)
ISN 0035      400 FORMAT(' MACE(X) (CM/DAY) ',8(E12.4,2X))
ISN 0036      WRITE(6,450)(MMENE(I),I=1,NSL)
ISN 0037      450 FORMAT(' MMENE (CM/DAY) ',8(E12.4,2X))
ISN 0038      WRITE(6,500)(DBETA(I),I=1,NSL)
ISN 0039      500 FORMAT(' BETA/DL(ML/ML) ',8(E12.4,2X))
ISN 0040      WRITE(6,600)(DBET(I),I=1,NSL)
ISN 0041      600 FORMAT(' DBET/DL(ML/ML) ',8(E12.4,2X))
ISN 0042      WRITE(6,700)(DTET(I),I=1,NSL)
ISN 0043      700 FORMAT(' THETA/DL(ML/ML) ',8(E12.4,2X))
ISN 0044      C SET UP MONTHLY WATER ACCOUNTS
ISN 0045      DO 800 J=1,NSL
ISN 0046      MMAME(J)=MMAME(J)+DMAME(J)
ISN 0047      DMAME(J)=0.0
ISN 0048      MMENE(J)=MMENE(J)+DMENE(J)
ISN 0049      DMENE(J)=0.0
ISN 0050      MMENA(J)=MMENA(J)+DMENA(J)
ISN 0051      DMENA(J)=0.0
ISN 0052      MMACEX(J)=MMACEX(J)+MACE(X)
ISN 0053      MACE(X)=0.0
ISN 0054      800 CONTINUE
ISN 0055      RETURN

```

WSWIFT (Continued)

```

C      MONTHLY WATER STATUS
ISN 0045  ENTRY 1MONTH
ISN 0046  WRITE(6,105)
ISN 0047  105  FORMAT(16X,' MONTHLY WATER BUDGETS   ')
ISN 0048  WRITE(6,110)(MMNAME(I),I=1,NSL)
ISN 0049  110  FORMAT(' MMNAME (CH/PTH) ',8(E12.4,2X))
ISN 0050  WRITE(6,210)(MMERA(I),I=1,NSL)
ISN 0051  210  FORMAT(' MMERA (CH/PTH) ',8(E12.4,2X))
ISN 0052  WRITE(6,310)(MMAPM(I),I=1,NSL)
ISN 0053  310  FORMAT(' MMAPM (CH/PTH) ',8(E12.4,2X))
ISN 0054  WRITE(6,410)(MMACEX(I),I=1,NSL)
ISN 0055  410  FORMAT(' MMACEX(CH/PTH) ',8(E12.4,2X))
ISN 0056  WRITE(6,510)(MMERE(I),I=1,NSL)
ISN 0057  510  FORMAT(' MMERE (CH/PTH) ',8(E12.4,2X))
ISN 0058  DO 900 J=1,NSL
ISN 0059  MMNAME(J)=0.0
ISN 0060  MMERA(J)=0.0
ISN 0061  MMAPM(J)=0.0
ISN 0062  MMACEX(J)=0.0
ISN 0063  MMERE(J)=0.0
ISN 0064  900  CONTINUE
ISN 0065  RETURN
ISN 0066  END

```

NOMENCLATURE

SOURCE OF OUTWARD

$${}^t\text{FLOW}(K) = (\text{surface area of macropore})(\text{height of water in macropore}) \\ (\text{hydraulic conductivity})(\text{hydraulic gradient})(\text{number of macropores})^*$$

Height of water in macropores (cm):

$${}^t\text{HMAT}(K) = \text{macropore water content}^*/(\text{macroporosity})(\text{fraction of macropores}^*)$$

Hydraulic gradient from macropore to mesopores (cm water/cm):

cylindrical pore: ${}^t\text{HGRAD}(K) = (\text{mesopore matric potential} + \text{average macropore potential})/[\text{macropore radius} \cdot \ln(\text{distance from macropore to mesopores}/\text{macropore radius})]$

rectangular crack: ${}^t\text{HGRAD}(K) = (\text{mesopore matric potential} + \text{average macropore potential})/(\text{distance from macropore to mesopores})$

Total number of macropores:

$$\text{NPOR}(K) = \text{macroporosity}(\text{length of soil layer})/\text{macropore volume}$$

$$\text{macropore volume: A-horizon} = (\pi)(\text{pore radius})^2(\text{length of macropore})$$

$$\text{B-horizon} = (\text{width})(\text{breadth})(\text{length of crack})$$

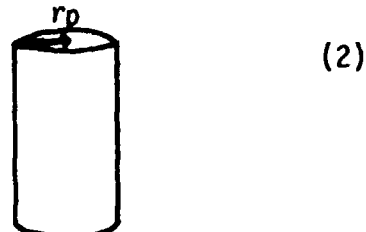
^tSimilar for dead-end macropores.

^{*}Either continuous or dead-end macropores, depending on calculation.

10.4 Calculation of Maximum Flow Rate Through Macropores

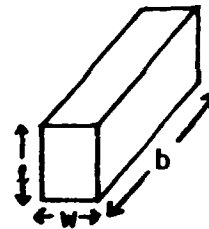
From Poiseuille's Law, the flow in a cylinder is given by:

$$q_p = \frac{\pi \Delta P}{8\mu} (r_p^4)$$



Similarly, flow in slits may be expressed as:

$$q_c = \frac{2}{3} \frac{\rho g}{\mu} w^3 b$$



(3)

where

 ρ = density of fluid g = acceleration due to gravity μ = dynamic viscosity of fluid q_p = flux in cylindrical pores q_c = flux in cracks r_p = radius of a cylindrical pore w = width of a rectangular crack b = breadth of a rectangular crack

Tables 2 and 3 show the flux through macropores of different dimensions for cylindrical pores and rectangular cracks, respectively.

Table 2. Flow Through Cylindrical Pores as Determined by Poiseuille's Law

r_p (cm)	Number of Macropores N_p	q_p (cm ³ /h)	Macroporosity
0.04	1	355	0.005
0.04	10	355×10^1	0.05
0.40	1	355×10^4	0.50

Table 3. Flow Through Cracks as Determined by Poiseuille's Law

w (cm)	b (cm)	z (cm)	N_p	q_c (cm ³ /h)	Macroporosity
0.005	1.0	1.0	1	29.4	0.005
0.05	1.0	1.0	1	29.4×10^3	0.05
0.05	1.0	1.0	10	29.4×10^4	0.50

Note that macroporosity does not enter into the calculation of q_p or q_c . It is shown here only for comparison.

The precipitation rate was compared with the maximum flow rate possible through macropores. Precipitation records have shown rainfall rates up to $30 \text{ cm}^3 \cdot \text{cm}^{-2} \cdot \text{h}^{-1}$ in some tropical regions; however, these rates are exceptional and a more typical high rainfall rate would be $6 \text{ cm}^3 \cdot \text{cm}^{-2} \cdot \text{h}^{-1}$. These high rainfall rates are much lower than the maximum flow rates (q_p , q_c) shown in Tables 2 and 3. Therefore, the flow in macropores will not be limited by pore geometry but rather by macropore capacity.

10.5 Pore Size Distribution

Macropores are pores where capillary forces are negligible or flow is not appreciably affected by these forces. Macropores are somewhat arbitrarily defined to be pores which are filled with water at suctions less than 10 cm of water. The radius corresponding to 10 cm of suction is calculated using the expression for capillary pressure (7):

$$p = \frac{2\delta \cos \alpha}{R} \quad (4)$$

where δ is the surface tension, α is the contact angle in a capillary, and R is the radius of the capillary, which leads to,

$$R = \frac{2\delta \cos \alpha}{\rho g H} \quad (5)$$

where ρ is the density of manometer fluid and H is the height of the fluid. Some calculations for different heights of suction are shown in Table 4.

Table 4. Radius of Pores for Different Heights of Suction

<u>H (cm)</u>	<u>R (cm)</u>
0.05	3.00
5	0.03
10	0.015
20	0.0075

A minimum macropore radius of 0.015 cm is obtained for a suction of 10 cm of water in soil. Although apparently small, this value for a radius will account for the few small macropores. The mesopores should be of a much smaller size. For rectangular cracks, $1/w$ is substituted for $2/R$, giving a minimum crack width of 0.0075 cm.

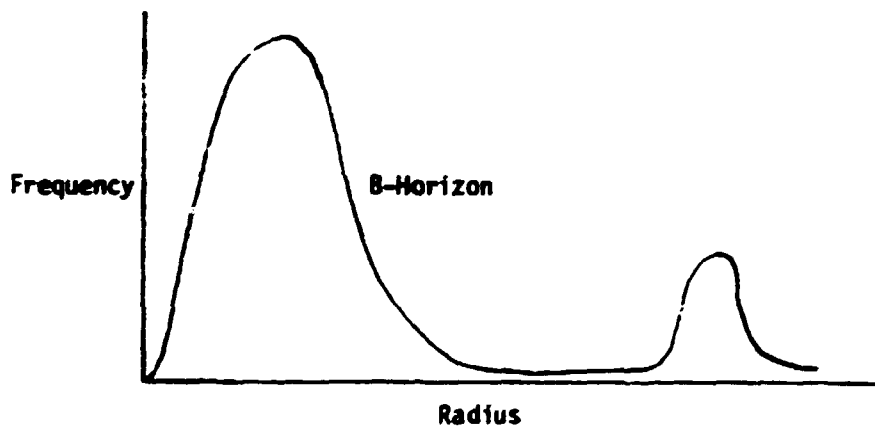
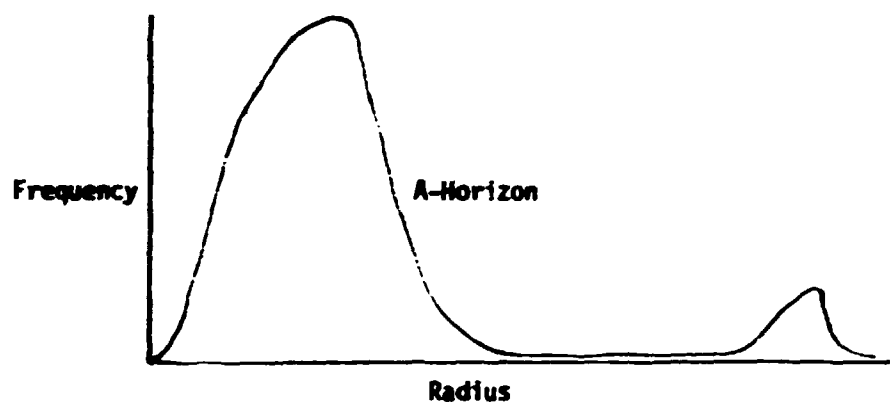
A Gaussian-type of distribution with separate peaks for mesopores and macropores was assumed for the pore sizes in each horizon. A schematic diagram of the expected frequency distribution is shown in Fig. 11.

In the A-horizon, the mesopore distribution may be skewed towards higher radii because of the larger size of soil particles than those found in the B-horizon (1). The same tilt may occur for macropores, since the few of them which arise from biological forces are generally larger than those which arise from physical forces.

From drainage tests conducted at the field soil-block facility, mesopore size distributions at different depths into the soil were derived. The field facility was a 2x2-m soil block, with rubber lining down to 2 m on three sides and a concrete wall down to 3 m on the fourth side, as shown in Fig. 12. Soil moisture content was measured by neutron scattering from a neutron probe placed at selected positions within each of two access tubes located 1 m apart. On the concrete wall, access ports were situated at different depths for tensiometers that measured soil water potential. From the data of the two types of instruments obtained during drainage of the flooded soil block, the relationships between water content and water potential (retention curves) were developed for selected depths. A distinctive change in drainage from the A- to B-horizon (37-cm depth), as seen in Fig. 13, may account for surface ponding or the perched water table during winter. The water content-potential curve showed a discrepancy between the field and the laboratory data (Fig. 14). This may be attributed to entrapped air in the field soil sample. In the field, the soil is flooded from the top while the soil in the laboratory is wetted upward from the bottom.

Mesopore size distributions were calculated from the field data with the assumption that the mesopores were spherical. A comparison between the distributions for the same location but at different depths is shown in Fig. 15.

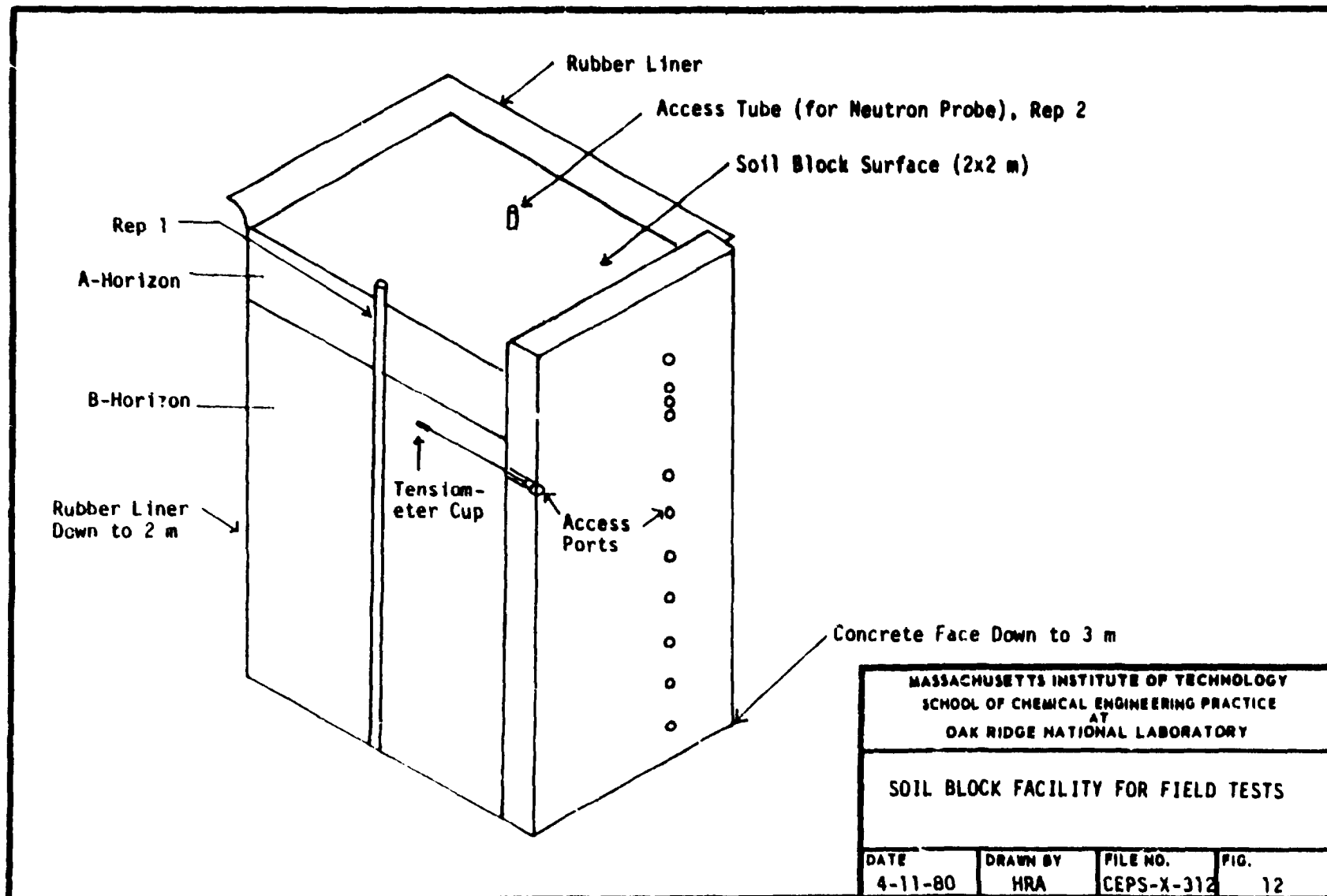
Contrary to expectations, the normalized distribution curve at the higher level skewed towards higher radii. Another comparison between the distributions for the same depth (10 cm), but two locations one meter apart (different reps) is shown in Fig. 16. From these two figures, we can conclude that a wide variation in the frequency distribution not only exists between different locations in the soil, but also between different levels in the same profile. It is obvious from the two figures that the distribution did not cover the entire pore size range. Exclusion of the macropore distributions resulted from calculations of the radii which were based on the rise of water in the manometer due to capillary effects. Small pores of radii less than ~0.004 cm were not analyzed in this method because they had not drained in the time interval considered (~55 days).



MASSACHUSETTS INSTITUTE OF TECHNOLOGY
SCHOOL OF CHEMICAL ENGINEERING PRACTICE
AT
OAK RIDGE NATIONAL LABORATORY

EXPECTED RELATIVE PORE SIZE
DISTRIBUTIONS IN A- AND B-HORIZONS

DATE	DRAWN BY	FILE NO.	FIG.
4-14-80	HKA	CEPS-X-312	11



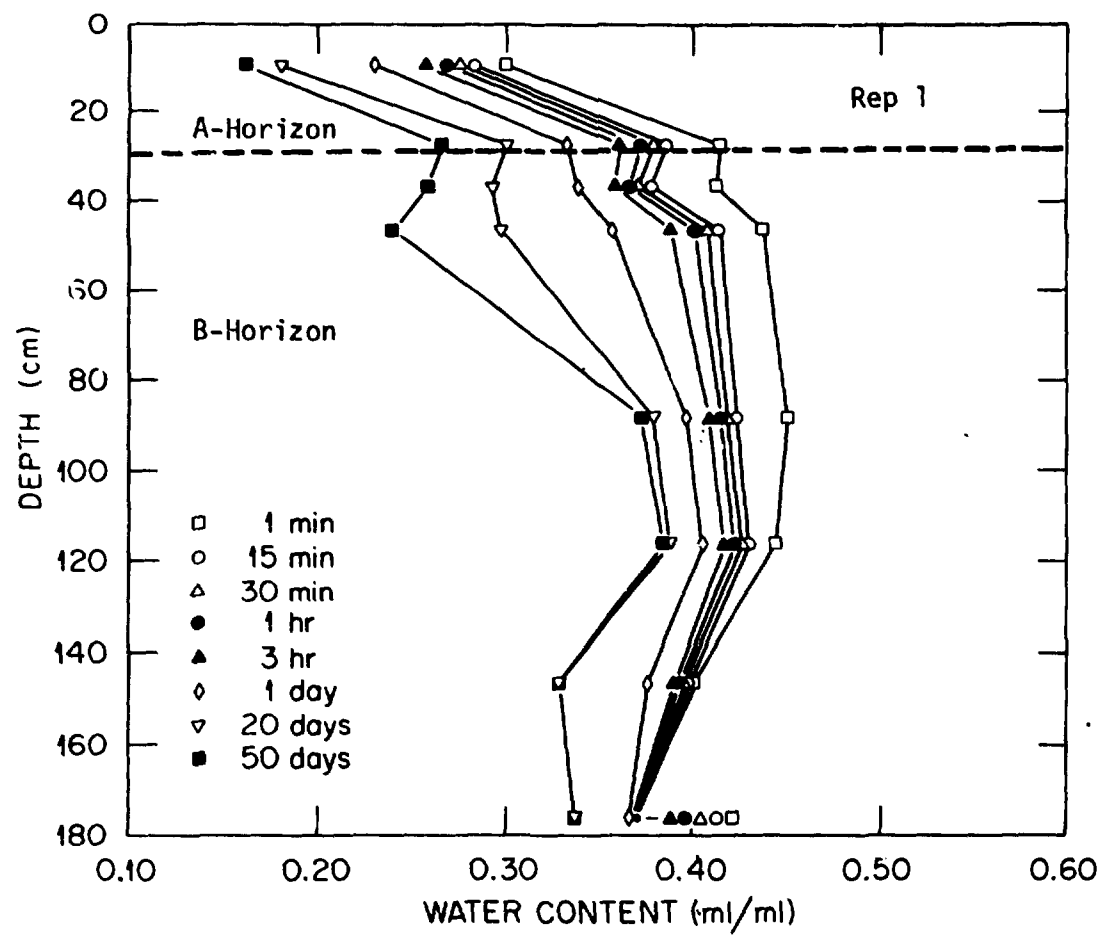


Fig. 13. Water Content Profile (11)

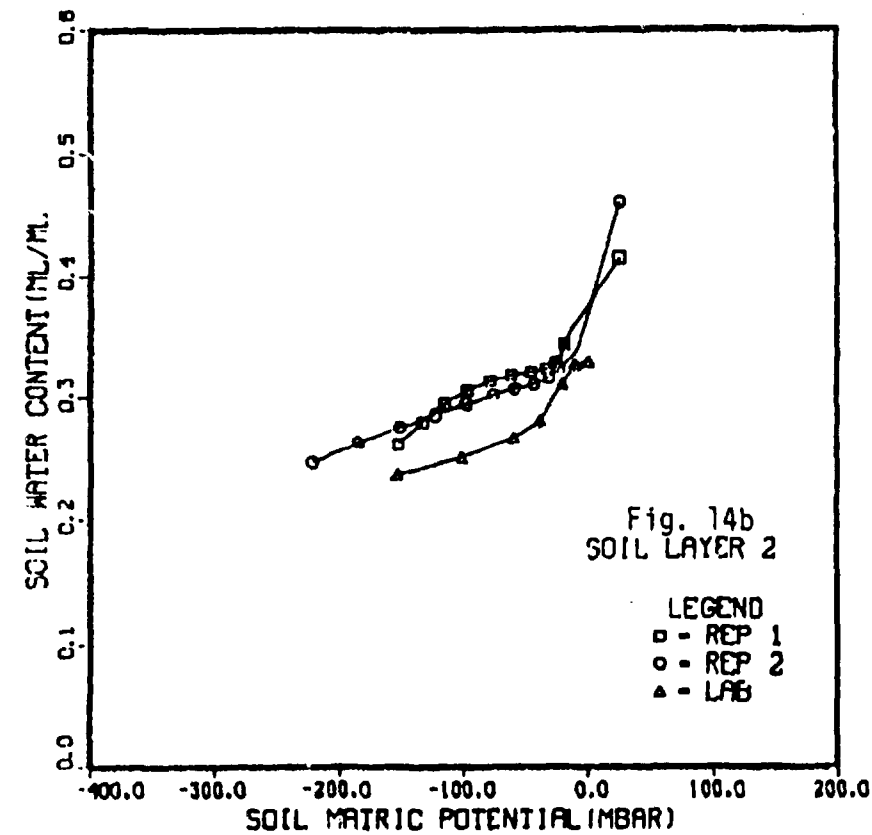
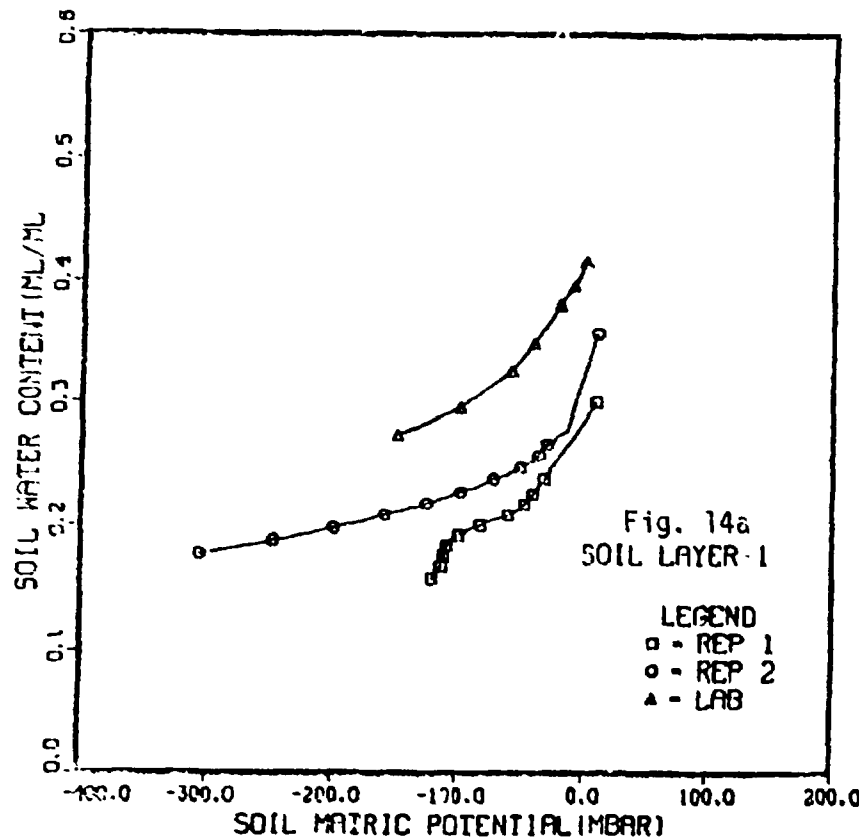


Fig. 14. COMPARISON OF LABORATORY AND BLOCK FACILITY WATER RETENTION DATA (11)

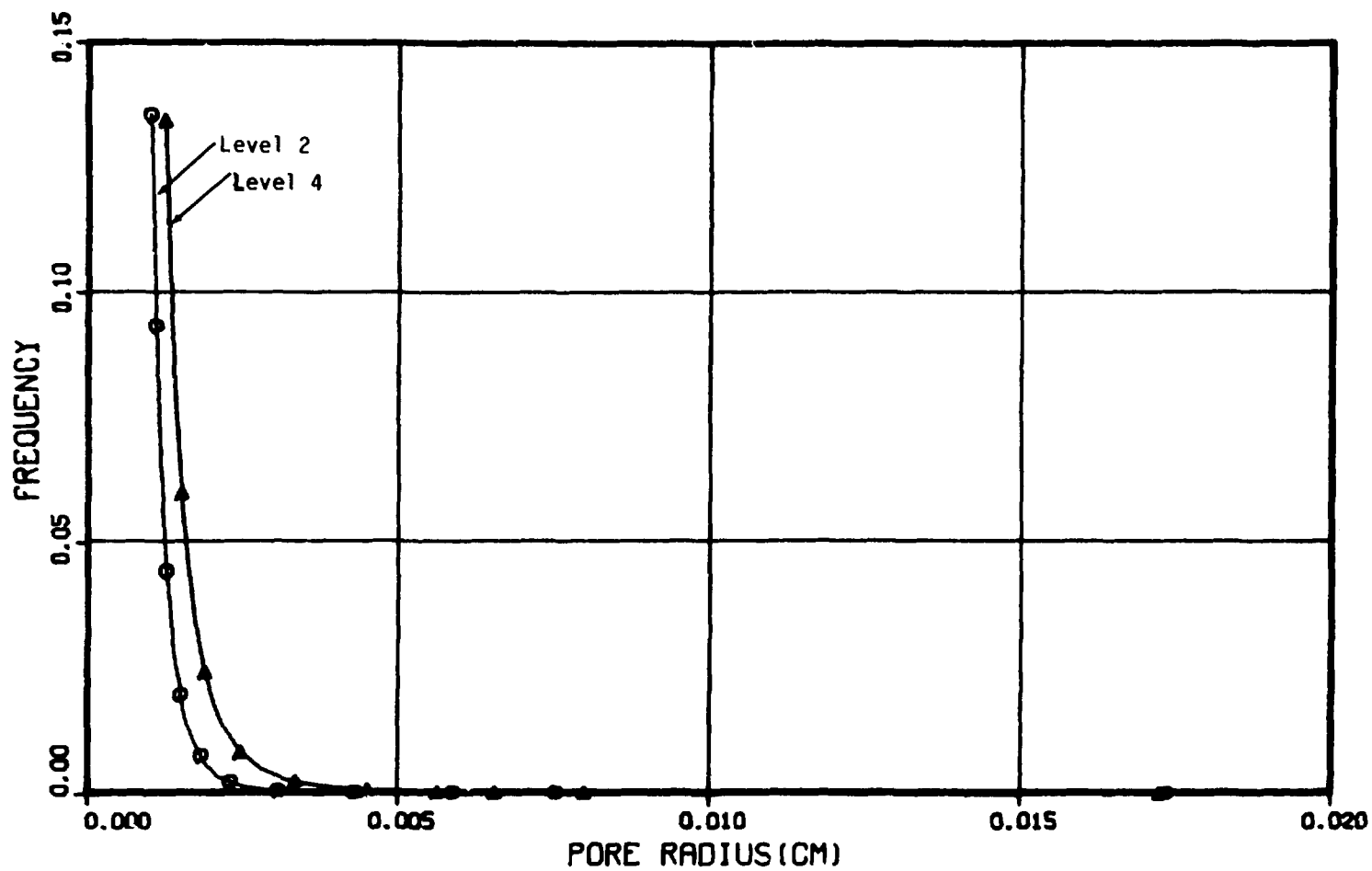


Fig. 15. MESOPORE SIZE DISTRIBUTION AT DIFFERENT DEPTHS (Rep 1)

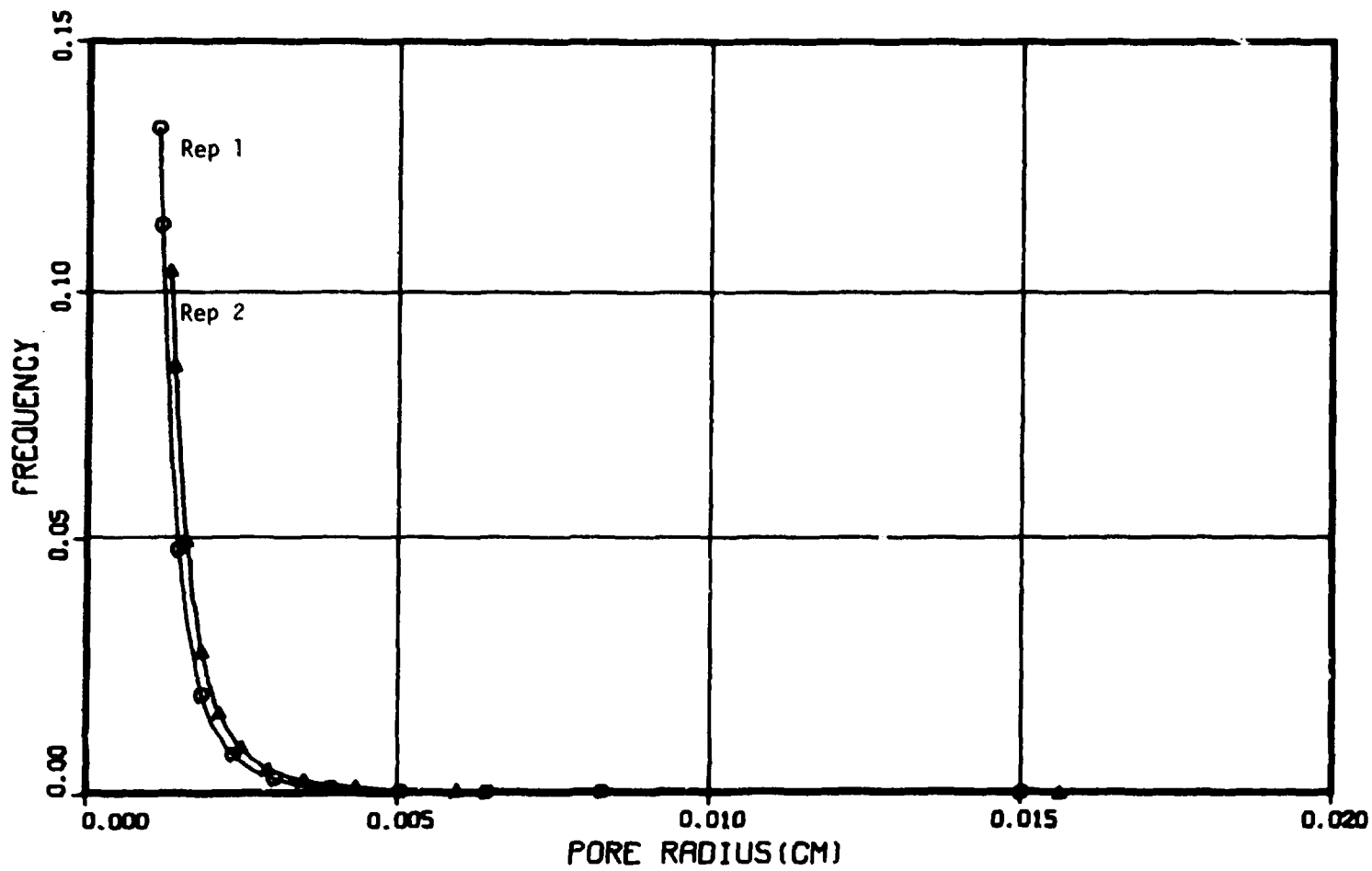


Fig. 16. Mesopore Size Distribution at Different Lateral Positions (Level 3)

A flowchart of the algorithm used for calculating mesopore size distributions is given in Fig. 17, with the diagram being followed by the FORTRAN logic employed.

The pore size frequency distributions for 6 levels (10, 28, 37, 47, 89, and 117-cm depth) at two locations (Rep 1 and Rep 2) (Figs. 18 and 19) in Fullerton cherty silt loam soil were calculated by the method reported by Marshall (12) from soil water content-potential relationships obtained from the field soil (11). The results showed that there were very few pores with radius greater than 0.01 cm and that the smallest pore size was the most frequent class.

10.6 Documentation of Inputs

Additional inputs into TEHM:

macroporosity (MCPOR)

proportion of dead-end macropores (PERC)

radius of cylindrical pores (RP)

width of cracks (WP)

breadth of cracks (PL)

length of aggregate (AGSIZE)

flag for YESMAC:

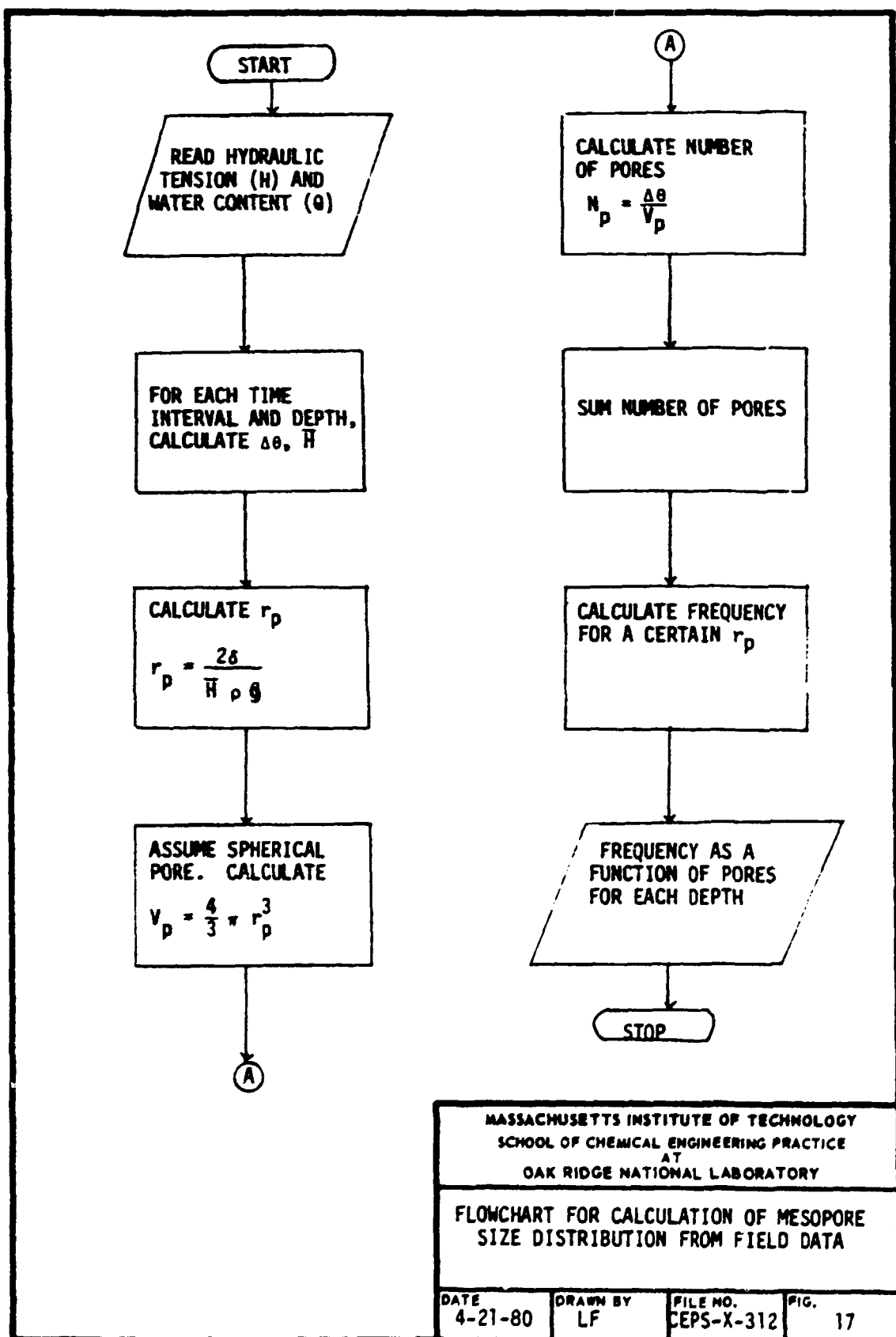
YESMAC = 0 for no macropore effects

YESMAC = 1 for macropore effects

A section of a sample input data file is given on page 47.

Documentation:

<u>Subroutine</u>	<u>Card Number</u>	<u>Columns</u>	<u>Description of Input Data</u>
READIN	7.11	30 - 40	FORMAT (2G10.3, 2I5, F10.0) YESMAC; flag for macropore flow effects YESMAC = 0 for no macropores YESMAC = 1 for macropores
RSWIFT (called from READIN)	7.53 to 7.32 + NSL	1 - 10 11 - 20	FORMAT (6F10.4) One card per soil layer for NSL soil layers MCPOR; macroporosity in that layer, ml/ml RP; radius of cylindrical pores if in A-horizon, cm (put 0.0 for B-horizon)



PORE SIZE DISTRIBUTION FORTRAN PROGRAM

```

COMPILER OPTIONS - NAME= MAIN,OPT=02,LINECNT=60,SIZE=0000K.
      SOURCE,EBCDIC,NOLIST,NOECK,LOAD,NAP,NOEDIT,IO,NOXREF

      C      CALCULATION OF MESOPORE SIZE DISTRIBUTION ASSUMING SPHERICAL
      C      PORES
      C
      C      DIMENSION THETA(51,8),H(51,8)
      C      DIMENSION PH(51,8),RP(51,8),RNP(51,8),T(51),TIME(51),SUM(8)
      C      DATA SIGMA,PH0/73.5,1.0/
      C      G=980.1
      C      PHI=3.1416

      C      READ HYDRAULIC TENSION AND WATER CONTENT DATA
      DO 2  I=1,51
      READ(5,100) T(I),(H(I,J),J=1,8)
      FORMAT(2X,F8.4,8F6.1)
      DO 4  I=1,51
      READ(5,200) T(I),(THETA(I,J),J=1,8)
      FORMAT(1X,F9.5,8F5.4)

      C      WRITE HEADINGS FOR OUTPUT DATA
      DO 10  J=1,8
      WRITE(6,500)
      WRITE(6,600) J
      FORMAT(30X,'LEVEL ',I2)
      WRITE(6,300)
      FORMAT(8X,'TIME',9X,'PORE RADIUS',7X,'FREQUENCY',10X,'NUMBER')
      WRITE(6,500)
      FORMAT(' ')
      C

      ISM 0013      SUM(J)=0.0
      ISM 0014      DO 6  I=1,50
      ISM 0015      C      SKIP NEGATIVE OR INCONSISTENT DATA
      ISM 0016      IF (H(I,J)<0.0)  GO TO 6
      ISM 0017      IF (THETA(I+1,J)>=THETA(I,J))  GO TO 12
      ISM 0018      DTHETA=THETA(I,J)-THETA(I+1,J)
      ISM 0019      GO TO 14
      ISM 0020      DTHETA=0.0
      ISM 0021      AVH=(H(I+1,J)+H(I,J))/2.0-1.5
      ISM 0022      C

      ISM 0023      C      CALCULATE RADIUS OF PORE CORRESPONDING TO THAT HYDRAULIC TENSION
      ISM 0024      RP(I,J)=(2*SIGMA)/(AVH*PH0*G)
      ISM 0025      VP=4.0/3.0*PHI*RP(I,J)**3
      ISM 0026      C

      ISM 0027      C      CALCULATE NUMBER OF PORES CORRESPONDING TO THAT RADIUS
      ISM 0028      PN(I,J)=DTHETA/VP
      ISM 0029      SUM(J)=SUM(J)+PN(I,J)
      ISM 0030      TIME(I)=(T(I+1)+T(I))/2.0
      ISM 0031      C

      ISM 0032      C      WRITE PORE RADIUS, FREQUENCY AND PORE NUMBER
      ISM 0033      DO 8  I=1,50
      ISM 0034      RNP(I,J)=PN(I,J)/SUM(J)
      ISM 0035      WRITE(6,400) TIME(I),RP(I,J),RNP(I,J),PN(I,J)
      ISM 0036      FORMAT(F13.4,9X,F8.6,8X,E10.4,9X,E10.4)
      ISM 0037      400      CONTINUE
      ISM 0038      8
      ISM 0039      400
      ISM 0040      10      STOP
      ISM 0041      END
      ISM 0042

```

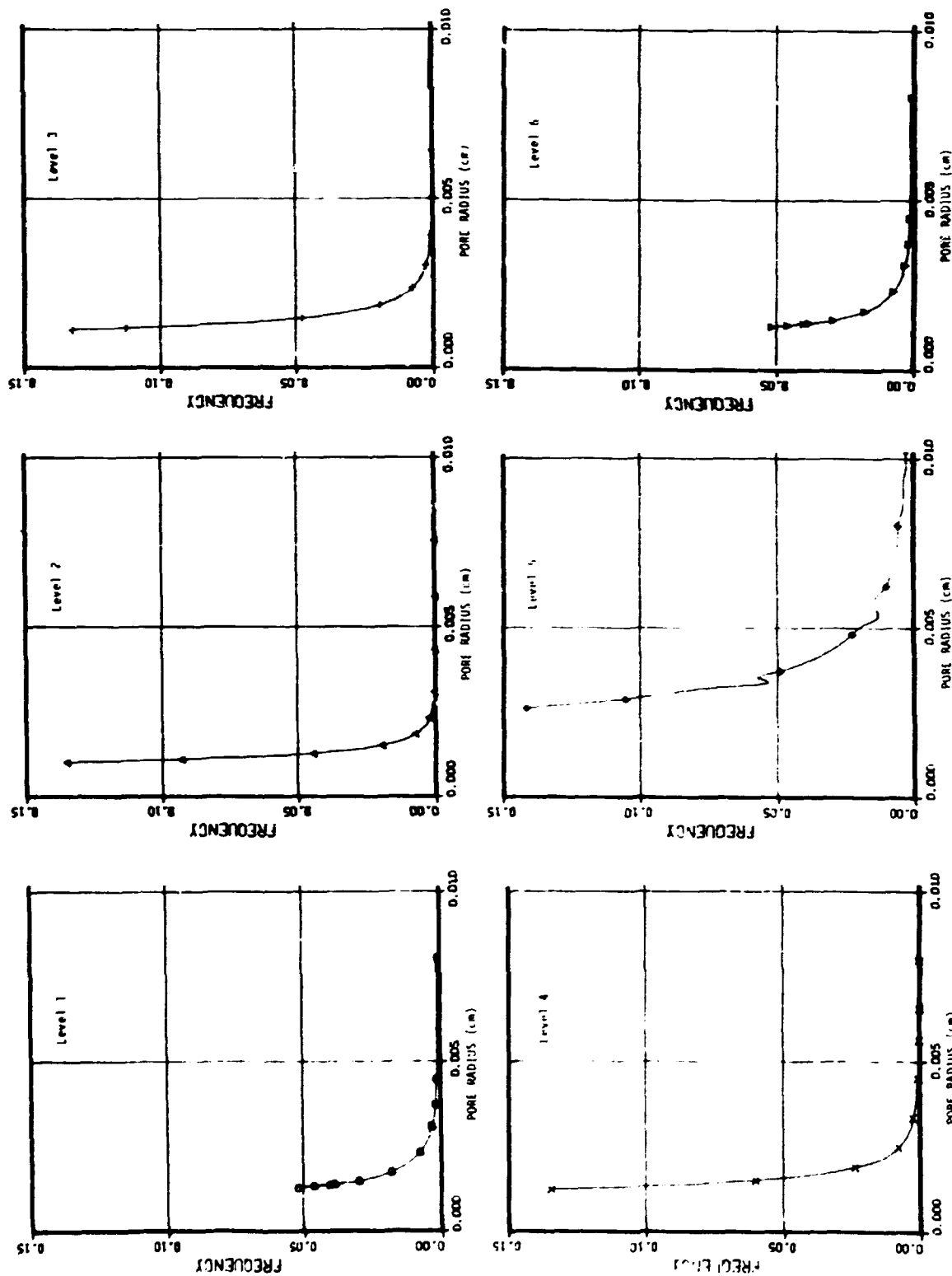


FIG. 1A. Mesh pore size distribution for six levels of Rep 1

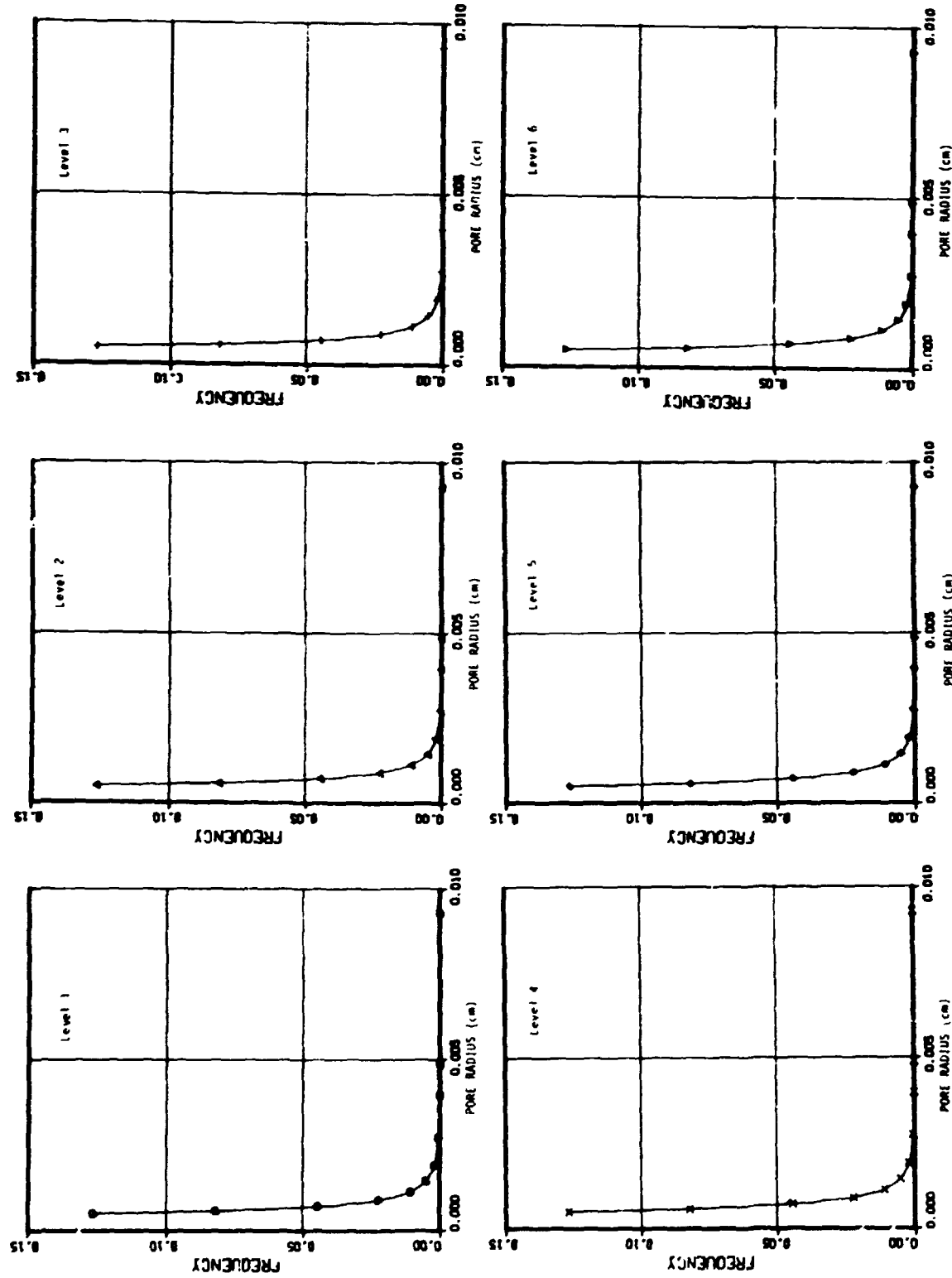


Fig. 19. Metapore Size Distribution for Six Levels of Rep 2

Sample Input Data

7 PROSPER READIN ---- ANALYSIS: MACROPERMEABILITY(0.04)

1 DATA AND SIMULATION OF WALKER BRANCH WATERSHED

30.0	60.0	60.0	60.0	60.0	
.1591	.2666	.2466	.2466	.2466	
.308					
1.0132	.24	10.	100.	1.0	
.2	.01	.6	.4	20.	
6.001	6.3	0.0	20.		
500000.	.001	.001			
129.	139.	260.	306.		
2.0	8.0	2.	1.	.12	.16
0.6	0.48	5	3	1.	
34.	8.	250.	250.	-0.5	-0.5
0.0	180.	36.0			

FULLEPTON A2/E WALKER BRANCH

9	50	.27	9.6	0.0	
73.49	0.999	.01138	15.	980.	
2.0					
.125.143.159.170.187.210.240.263.270					
11900.	3950.	790.	527.	263.	79.0
19.8	3.95	0.			

FULLEPTON B21/6 WALKER BRANCH

9	50	.246	4.8	0.0	
73.49	0.999	.01138	15.	980.	
2.0					
.166.177.187.193.201.211.225.236.246					
11900.	3650.	790.	527.	263.	79.0
19.8	3.95	0.			

FULLEPTON B22T/6 WALKER BRANCH

9	50	.304	4.8	0.0	
73.49	0.999	.01138	15.	980.	
2.0					
.184.198.211.218.226.257.278.298.304					
11900.	3650.	790.	527.	263.	79.0
19.8	3.95	0.			

INFILTRATION CURVE/6 FOREST SOIL

15.	0.0	0.0	25													
0.	.324	.648	.949	1.26	1.57	1.89	2.20	2.51	2.82	3.14	3.45	3.76	4.07	4.38	4.69	
4.99	5.30	5.60	5.51	6.22	6.52	6.82	7.12	7.41								
0.	2.67	4.94	7.41	5.88	12.4	14.8	17.3	19.8	22.2	24.7	27.2	29.6	32.1	34.6	37.0	
34.5	42.0	44.5	46.9	49.4	51.9	54.3	56.8	59.3								
0.04	0.25	0.00	0.00	0.10	0.00											
0.04	0.25	0.00	0.00	0.10	0.00											
0.04	0.00	0.0625	1.00	0.05	2.00											
0.04	0.00	0.0625	1.00	0.05	2.00											
0.04	0.00	0.0625	1.00	0.05	2.00											

Input for MCPOR, RP, WP, PL, PERC, AGSIZE (in order)

8 SUBSURFACE PARAMETERS

C.00	10.	1.0	0.0	2.	
160.	180.				
.212	.212				
.29:4536730.226.06886202.134142.1391	700.00104.5259	0.210	0.233		
0.02	0.12	0.00			

16 GC

7 1 59 59

6 LAMPAD COL 9-90 FOR COMMENTS. SEE M26

1.0	0.00	25.	0.24	0.4	
0.12	0.072				
1	4	2			

7 PROSPER READIN ---- ANALYSIS: VESOPORES ONLY(YESMAC=0.0)

1 DATA AND SIMULATION OF WALKER BRANCH WATERSHED

30.0	60.0	60.0	60.0	60.0	
.1591	.2666	.2466	.2466	.2466	
.308					

Documentation (continued):

<u>Subroutine</u>	<u>Card Number</u>	<u>Columns</u>	<u>Description of Input Data</u>
RSWIFT		21 - 30	WP; width of cracks if in B-horizon, cm (put 0.0 for A-horizon)
		31 - 40	PL; breadth of cracks if in B-horizon, cm (put 0.0 for A-horizon)
		41 - 50	PERC; proportion of dead-end macropores
		51 - 60	AGSIZE; average length of aggregate size, cm

10.7 Input Data Sets

Standard Case

<u>Layer</u>	<u>Porosity</u>	<u>Radius</u>	<u>Width</u>	<u>Breadth</u>	<u>Proportion of Dead-End Pores</u>	<u>Length</u>
1	0.05	0.25	0.00	0.00	0.10	0.0
2	0.05	0.25	0.00	0.00	0.10	0.0
3	0.10	0.00	0.0625	1.00	0.05	2.0
4	0.10	0.00	0.0625	1.00	0.05	2.0
5	0.10	0.00	0.0625	1.00	0.05	2.0

Each of the following data sets contains seven cases with one parameter being varied from the standard value for each case.

For Hydraulic Conductivity and Porosity Study

SENYES.DAT Hydraulic Conductivity: Layer 1 - 240 cm/d; Layers 2-5 - 120 cm/d

Macroporosity

1	0.04	5	0.02
2	0.00	6	0.08
3	0.005	7	YESMAC = 0 (ignore macropores)
4	0.01		

SLOW.DAT Hydraulic conductivity: Layer 1 - 9.6 cm/d, Layers 2-5, 4.8 cm/d

Macroporosity

1	0.00	5	0.02
2	0.08	6	0.04
3	0.005	7	YESMAC = 0 (ignore macropores)
4	0.01		

Additional Sensitivity Analysis

TEST.DAT Hydraulic conductivity: Layer 1 - 9.6 cm/d; Layers 2-5, 4.8 cm/d

Macroporosity = 0.04 for each case

1	width = 0.10	5	proportion of dead end = 0.0
2	standard macroporosity = 0.04	6	radius = 0.025
3	macroporosity = 0.16	7	width = 0.01
4	proportion of dead end = 0.20 + 0.10		

For Detailed Sensitivity Analysis (suggested)

ANAL1.DAT

Macroporosity	Proportion of dead-end pores
1 0.04	5 0.00
2 0.08	6 0.05
3 0.12	7 0.25
4 0.16	

ANAL2.DAT

Proportion of dead-end pores	Radius	Width
1 0.50	2 0.015	5 0.0075
	3 0.150	6 0.0750
	4 1.500	7 0.7500

ANAL3.DAT

Breadth	Length	Macroporosity
1 0.5	4 0.50	7 0.10, 0.05
2 2.0	5 1.00	
3 5.0	6 5.00	

ANAL4.DAT

Macroporosity	Proportion of Dead-End Pores
1 0.00	7 0.50
2 0.001	
3 0.005	
4 0.01	
5 0.02	
6 0.04	

10.8 Computer Variables

AGSIZE(K)	average length of an aggregate, cm
B(K)	capacity of continuous macropores, cm/layer
BD(K)	capacity of dead-end macropores, cm/layer
BETA(K)	water content of continuous macropores, cm/layer
BYPS	fraction of non-vertical flow through aggregates
DBET(K)	water content of dead-end macropores, cm/layer
DBETA(K)	daily water content of continuous macropores, ml/ml
DDBET(K)	daily water content of dead-end macropores, ml/ml
DFLOW(K)	flow from dead-end macropores to mesopores, cm/time increment
DHGRAD(K)	hydraulic gradient - mesopores to dead-end macropores, dimensionless
DHWAT(K)	height of water in dead-end macropores, cm
DL(K)	length of soil layer, cm

DMAMA(K)	daily macropore-to-macropore flow, cm/d
DMAME(K)	daily macropore-to-mesopore flow, cm/d
DMEMA(K)	daily mesopore-to-macropore flow, cm/d
DX(K)	distance from macropore to mesopore, cm
EXCESS	excess water from macropores, cm
FRAC	fraction of pore length over vertical distance, dimensionless
FLOW(K)	flow from continuous macropores to mesopore, cm/time increment
FLXMAX	maximum infiltration rate for first soil layer, cm/time increment
HGRAD(K)	hydraulic gradient - mesopores to continuous macropores, dimensionless
HWAT(K)	height of water in continuous macropores, cm
MACEX(K)	daily total of macropore excess, cm
MCPOR(K)	macroporosity, dimensionless
MFBL	macropore flow between layers, cm
MMAMA(K)	monthly macropore-to-macropore flow, cm/month
MMACEX(K)	monthly macropore excess, cm
MMAME(K)	monthly macropore-to-mesopore flow, cm/month
MMEMA(K)	monthly mesopore-to-macropore flow, cm/month
NPOR(K)	number of macropores
NSL	number of soil layers
PERC(K)	fraction of dead-end macropores, dimensionless
PI	π
PL(K)	breadth of rectangular crack, cm
POND	flag set to 1 if there is surface ponding
PRE	precipitation, cm/time increment
PSM(K)	matric potential in mesopores, cm
RAIN	precipitation which enters macropores or is runoff, cm/time increment

RLAT(K)	lateral flow, cm/time increment
RP(K)	radius of cylindrical macropore, cm
S(K)	capacity of mesopores, cm/layer
TBET(K)	total water content of macropores, cm/layer
THETA(K)	water content of mesopores, cm/layer
TRUNO	surface runoff, cm/time increment
TWOPi	2π
WP(K)	width of rectangular crack, cm
YESMAC	flag set to zero if ignoring macropores
ZS(K)	hydraulic conductivity, cm/d
I, J, K	denotes I th , J th , or K th soil layer

10.9 Nomenclature

A	area of interaction, cm^2
b	breadth of rectangular crack, cm
g	gravitational constant, cm/s^2
H	height in a capillary, cm
K	hydraulic conductivity, cm/d
l	length of aggregate, cm
N _p	number of pores
P	capillary pressure
q _c	flux in cracks, cm^3/s
q _p	flux in cylindrical pores, cm^3/s
Q	flux of water in mesopore, cm^3/s
R	radius of a capillary, cm
r _p	radius of a pore, cm

V_p	volume of pores, cm^3
w	width of a rectangular crack, cm
x	average distance between macropores and mesopores, cm
α	contact angle in a capillary, degrees
δ	surface tension, g/s^2
θ	water content in mesopore, cm^3/layer
μ	dynamic viscosity, g/s-cm
ρ	density, g/cm^3
ψ	hydraulic potential, cm water

10.10 Literature Cited

1. Beven, K., and P. Germann, "Water Flow in Soil Macropores 2. A Combined Flow Model," OXON-OX10-888, Institute of Hydrology, Wallingford (1979).
2. Edwards, W.M., R.R. van der Ploeg, and W. Ehlers, "A Numerical Study of the Effects of Non-Capillary-Sized Pores Upon Infiltration," Soil Sci. Soc. Am. J., 43, 851 (1979).
3. Huff, D.D., R.J. Luxmoore, J.B. Mankin, and C.L. Begovich, "TEHM: A Terrestrial Ecosystem Hydrologic Model," ORNL/NSF/EATC-27, Oak Ridge National Laboratory, Oak Ridge, TN (1977).
4. Luxmoore, R.J., personal communication, ORNL, April 1980.
5. Nelson, W.R., and L.D. Baver, "Movement of Water Through Soil in Relation to the Nature of the Pores," Soil Sci. Soc. Am. J., 5, 69 (1941).
6. Radcliffe, D., T. Hayden, K. Watson, P. Cowley, and R.E. Phillips, "Simulation of Soil Water Within the Root Zone of a Corn Crop," Agronomy J., 72, 19 (Jan-Feb 1980).
7. Scheidegger, A.E., "The Physics of Flow Through Porous Media," 2nd ed., pp. 53-55, Macmillan, New York, 1960.
8. Shaffer, K.A., D.D. Fritton, and D.E. Baker, "Drainage Water Sampling in a Wet, Dual-Pore Soil System," J. Environ. Qual., 8(2), 241 (1979).
9. Thomas, G.W., and R.E. Phillips, "Consequences of Water Movement in Macropores," J. Environ. Qual., 8(2), 149 (1979).

10. Todd, D.K., "Groundwater," in Handbook of Applied Hydrology, V.K. Chow, editor, pp. 13-4/13-5, McGraw-Hill, New York, 1964.
11. Luxmoore, R.J., and T. Grizzard, "Hydraulic Properties of a Deciduous Forest Soil. I. Field and Laboratory Retention Characteristics," Submitted to Soil Sci. Soc. Am. J. (1980).
12. Marshall, T.J., "Relations Between Water and Soil," Technical Communication No. 50, Commonwealth Bureau of Soils, Harpenden, United Kingdom (1959).

10.11 Literature Surveyed

1. Bouma, J., and J.H.M. Wösten, "Flow Patterns During Extended Saturated Flow in Two, Undisturbed Swelling Clay Soils with Different Macrostructures," Soil Sci. Soc. Am. J., 43, 16 (1979).
2. Cheng, J.D., T.A. Black, and R.P. Willington, "A Technique for the Field Determination of the Hydraulic Conductivity of Forest Soils," Can. J. Soil Sci., 55, 79 (Feb. 1975).
3. Chow, V.K., ed., Handbook of Applied Hydrology, McGraw-Hill, New York, 1964.
4. Flühler, H., M.S. Ardakani, L.H. Stolzy, "Error Propagation in Determining Hydraulic Conductivities from Successive Water Content and Pressure Head Profiles," Soil Sci. Soc. Am. J., 40, 830 (1976).
5. Linden, D.R., "A Model to Predict Soil Water Storage as Affected by Tillage Practices," Ph.D. Thesis, Univ. of Minnesota (1979).